

### **Semi-diagnostic calculation of seasonal mean circulation in the Indian Ocean**

#### **3.1 Introduction**

The Indian Ocean circulation is very unique because of the change in wind pattern associated with the Indian monsoon and of the peculiar geographical settings. Many unique features of the Indian Ocean including the basin wide circulation were discussed in the introductory chapter. North of 10°S, the surface winds blow from the southwest during May-September and from the northeast during November-February. Accordingly the circulation of the Indian Ocean reverses twice during a year north of 10°S latitude. The Indian Ocean exhibits very high seasonal and intraseasonal variability, but it does not show much interannual variability compared to Atlantic and Pacific Oceans.

One of the major objectives of ocean modeling is to simulate the observed circulation and to understand the forcing mechanisms. At any instant of time, the observed 3-dimensional circulation in the Indian Ocean is controlled by the local and remote forcings, and it is essential to identify the role of each forcing on the observed circulation in the monsoonal area. The main local forcing to be considered in any mathematical model of the circulation of Indian Ocean are the local surface wind and the variation of internal density field in the model area. The first large scale model of Indian Ocean developed by Cox (1970) showed that the rapid spin-up of Somali current at the beginning of the southwest monsoon was due to the local winds and later it was inferred that the local forcing is important initially, and the remote forcing effect becomes important over time. The semi-annual reversal of wind also generate large scale propagating signals such as Kelvin and Rossby waves. Investigations suggest that

these waves influence the dynamics of both the Bay of Bengal and the Arabian Sea (McCreary et al. 1993; Potemra et al., 1991). It is essential to identify the role of each of the above mentioned forcing on the observed circulation of the Indian Ocean. This is possible only by developing a hierarchy of mathematical models such as diagnostic, semi-diagnostic, prognostic and inverse models of circulation.

In a diagnostic model, all the equations of prognostic model except equations of temperature and salinity are used to study the steady state circulation of a particular area. In diagnostic models of ocean circulation, the internal density field is imposed on the model from the observations of temperature and salinity and is not predicted as part of the model calculation. The equation of state is used only to calculate the density field at different layers. Hence diagnostic modeling technique can be employed only in those regions of the oceans where observed data on temperature and salinity are available at regular spatial grids; in addition, the density field is kept constant throughout the model integration and only the steady state response of the sea to steady surface wind and internal density field, is studied. However, the diagnostic calculations are not very good if the density field is greatly smoothed or the density field contains significant errors or noises. Another drawback of the diagnostic model is that the imposed density field is not in adjustment with wind stress, flow field, bottom topography and the processes of advection and diffusion.

To overcome the drawbacks of diagnostic models, Sarkisyan and Demin (1983), for the first time, developed a new technique called, semi-diagnostic technique, to calculate the steady state 3-dimensional circulation. In a semi-diagnostic model, the adjustment of the observed data with model equations, boundary conditions and basin geometry takes place. The numerical solution of the semi-diagnostic models are completed in two stages; the first stage is called the diagnostic stage and the second stage is called adaptation or adjustment. In the diagnostic

state, only the equations of momentum (x and y momentum), hydrostatics, continuity and the equation for the integral function are solved subject to proper boundary and initial conditions. The initial state for the velocity field is a state of rest. The surface wind field is steady and is not interpolated at each time step of model integration. The diagnostic computations are continued only till the flow field is generated and it is not essential to continue the computations till full steady state is reached. In the second stage, the equations of the diagnostic model together with the equations of heat and salt are again solved, utilizing the flow field derived from the first diagnostic state and original temperature and salinity fields as initial conditions. The boundary conditions for temperature and salinity which are steady during the model integration are also to be incorporated as temperature and salinity equations are added during the adaptation stage. The integration of the full system of equations are again continued for another one month during which the observed density field is allowed to vary to a certain extent such that flow fields are hydrodynamically adjusted with the wind stress, bottom topography and the processes of advection and diffusion. The complete details about the semi-diagnostic methods are given in the monograph of Marchuk and Sarkisyan (1988).

This chapter addresses the problem of understanding the relative roles of steady local forcing of wind and internal density field in driving the circulation of the Indian Ocean using a semi-diagnostic model. The primitive equation type, sigma coordinate, 3-dimensional model, developed at the Institute of Numerical Mathematics, Russia, has been adapted and configured to the Indian Ocean area between the latitudes 36°S – 29.5°N and longitudes 22°E and 142°E. The peculiarities of the sigma coordinate model in semi-diagnostic mode, the forcing parameters of the model, results of calculation of steady state current and comparison of computed results and observed surface circulation are presented in this chapter. The dynamics of computed currents in terms of the local forcing considered in the model are also presented.

### **3.2 Features of sigma coordinate semi-diagnostic model of circulation**

Semi-diagnostic circulation models are generally used for the calculation of mean currents in the model area depending on the time scale of density and wind stress fields used. If the density and wind stress fields used in the model are monthly mean, then the solution of semi-diagnostic model would give the mean circulation for that particular month.

In the diagnostic stage, equations (2.15) – (2.18) together with the equations for the stream function (Eq.2.26) are solved subject to appropriate surface boundary conditions for wind stress components (Eq. 2.22) and other lateral and bottom boundary conditions given in Chapter II. The initial state is a state of rest ( $u = v = w = 0$ ), and the model was integrated for a period of two months when quasi-steady state was attained. In the second stage (adaptation stage), the above mentioned diagnostic model equations together with the equations for temperature and salinity (Eqns. 2.19 and 2.20) were again solved using the flow field obtained from the diagnostic stage and original temperature and salinity fields as initial conditions. At this stage, the surface boundary conditions for temperature and salinity ( $T = T_0$ ;  $S = S_0$ ) are to be incorporated. The integration of the above mentioned model equations were continued for another two more months during which the observed density field was allowed to vary such that flow fields were hydrodynamically adjusted with wind stress, bottom topography and the processes of advection and diffusion. During the adaptation stage, the noises in the initial temperature and salinity data were removed and steady state flow consistent with the model dynamics was generated.

### **3.3 Forcing parameters**

The basin wide surface wind field provides the major mechanical forcing for the upper hydrospheric structure, mass distribution and currents in the Indian Ocean. For the semi-diagnostic model, wind stress is main surface

forcing and hence a brief description of the wind field is presented first before presenting the results on currents. The presentation of spatial variation of forcing parameters would enable us to give meaningful interpretation to the results that were obtained from semi-diagnostic calculation. The climatological monthly mean wind stress ( $\text{dynes cm}^{-2}$ ) for January, July, April and October representing winter, summer, spring and autumn seasons respectively for the model area are presented in Fig. (2a-d).

South of  $10^{\circ}\text{S}$ , the southeast trades are present throughout the year. They have their seasonal maximum and maximum northerly extent during the southern winter. In the northern hemisphere, during winter, the monsoon winds are directed away from the Indian subcontinent, causing northeasterly wind stress over the Arabian Sea and Bay of Bengal. The strength of the northeasterly winds are high off the Somali region. These winds become weak at the equator and turn east after crossing the equator. During the southwest monsoon season (July), strong southeasterly winds are observed in the southern hemisphere between  $10^{\circ}\text{S}$  and  $30^{\circ}\text{S}$  latitudes. These winds turn southerly on approaching the equator and then turns southwesterly after crossing the equator. The main feature observed during the transition seasons are the occurrence of semi-annual eastward winds over the equator. These strong eastward winds are observed during April to June and October to November and it causes the annual mean equatorial zonal wind stress to be eastward.

### **3.4 Model circulation and comparison with observations**

Although, the semi-diagnostic model has 33 levels in the vertical at standard oceanographic depths, the computed results on currents for all the levels could not be presented in this chapter because of the enormity of the model output. The computed currents at the surface, 50 m, 150 m and 300 m depths only are presented in this chapter. Though the model

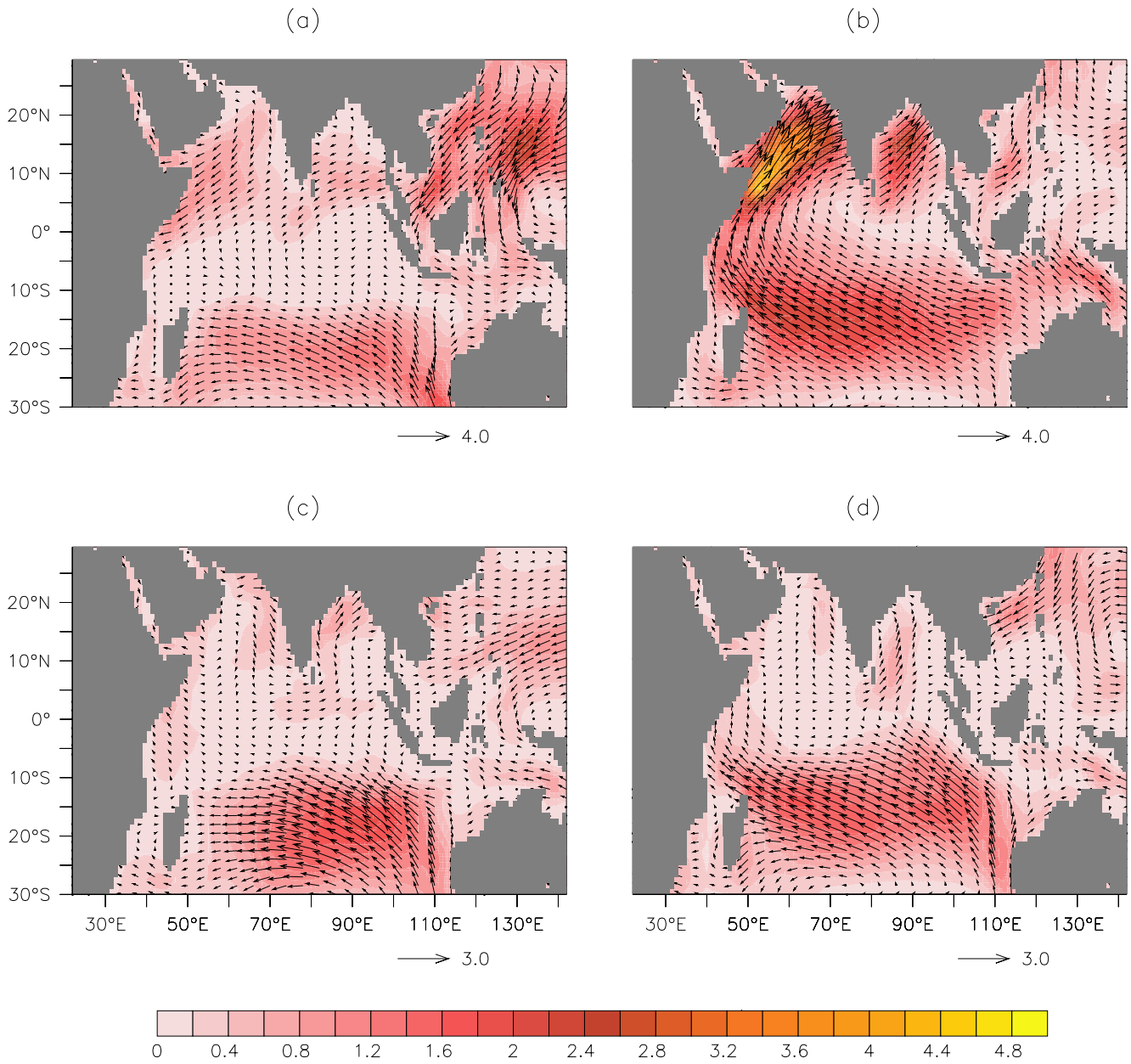


Fig.2 NCEP reanalysis wind stress fields for different months (dynes/cm<sup>2</sup>)

(a) January (b) July (c) April (d) October

area extends from 36°S to 29.5°N latitude, the mode I results are presented from 30°S to 29.5°N for convenience.

### **3.4.1 Spatial variability of mean current in the upper layers of Arabian Sea**

The main current systems observed in the Arabian Sea are essentially the reversing Somali Current (SC), the Southwest and North East Monsoon Current (SMC and NMC) and the West India Coastal Current (WICC). To describe the current structure over the entire annual cycle, it is essential to analyse in detail the variability of wind stress field including its curl fields for all the four cardinal months representing the main seasons of the year. During the summer monsoon, anticyclonic curl resides over most of the Arabian Sea and Equatorial Indian Ocean north of 15°S with its maximum over the central Arabian Sea to the right of the Findlater axis. The curl pattern reverses to cyclonic during the northeast monsoon. Over the western Bay of Bengal, the curl is cyclonic in summer and anticyclonic in winter.

The computed mean currents of the Indian Ocean at selected depths (upto 300 m) for the months of January, April, July and October, representing the four seasons of the year, are presented in Figs. 3.1 (a-d) to 3.4 (a-d). The steady state circulation (mean circulation) for each of the said particular month was obtained by integrating the semi-diagnostic model equations with the appropriate forcings of NCEP wind stress field and temperature salinity data (Levitus, 1994) for four months. The temperature and salinity data at selected depths (surface and 150 m. depths) for the months of January, April, July and October are also presented in Figs. 3.5 (a-b) to 3.12 (a-b) for a meaningful interpretation of the computed results. We begin with a review of the existing information on the dynamics of major current system in the Indian Ocean during the entire annual cycle and then discuss the results of our computations. Finally, based on the analysis of the forcing parameters and dynamical characteristics of the

model, the role of local forcing on the computed circulation would be discussed. Results of our computations will also be compared with available information on currents in the model area.

The seasonal development of the SC system was described by Schott et al. (1990). According to Schott et al. (1990), before the onset of monsoon during March-May, the southern Somali current is an extension of the East African Coastal Current (EACC) that flows northward across the equator to 3°N with a magnitude of 100 cm s<sup>-1</sup>. There it turns offshore forming a cold wedge along its shoreward side. With the monsoon onset in June, the cross equatorial flow strengthens to the order of 180 cm s<sup>-1</sup> and leaves the coast south of 4°N, where it partially turns eastward and partially flows back across the equator in a circulation pattern referred to as “Southern Gyre (SG)”. Another circulation, the “Great Whirl (GW)”, develops between 4°N – 12°N with a second cold wedge where it turns offshore. During October-November, when the southwest monsoon dies down, the cross equatorial SC turns offshore at 3°N with a magnitude of 130 cm s<sup>-1</sup>. The “Great Whirl” is even discernable underneath the developing northeast monsoon circulation well towards the end of the year. During the northeast monsoon season, the winds blow away from the Indian subcontinent and the surface Somali current reverses to flow southward. After crossing the equator, it encounters the northward flowing EACC, causing a confluence and eastward turnoff at 2-4°S. Until quite recently, few observations had been carried out in the northern Somali current during the winter monsoon. Moored arrays observations during WOCE 1995-96 (Schott and Fisher 2000) showed that the northern Somali current during this time was characterized by an inflow from the east, causing a divergence at the coast near 6-8°N, with a northward surface flow north of these latitudes and equatorward surface flow south of them. The northward surface flow passes through the Socotra passage, but also veers eastward along the southern banks of Socotra. The westward upper



layer flow into the Somali current system north of 7°N during winter is also confirmed by the XBT analysis of Donguy and Meyers (1995).

A number of modeling studies have attempted to simulate the Somali current response to the summer monsoon and to understand the process that cause it. Both local and remote forcing mechanisms have been proposed. The local is defined to be the direct driving by the alongshore component of coastal winds, and the remote forcing is any other processes. Remote forcing includes offshore winds that excite baroclinic Rossby waves that subsequently propagate to African coast, and several categories of waves that have been considered: (i) Equatorially trapped Rossby waves (ii) Rossby waves that radiate off the Indian coast and (iii) Rossby waves generated by wind stress curl offshore from Somali. A prominent example of the latter is the region of very strong negative wind curl on the eastern side of the Findlater jet; it is expected to drive an anticyclonic circulation, and several modeling studies suggested that the “Great Whirl” may be a directly forced response to this curl. Collectively, the studies indicate that the local forcing is the primary forcing mechanism of the summer time Somali current, but that remote forcing effects are also important significantly altering the coastal flows. Another important result is the realization of the dynamical importance of the north-south slope of the western boundary.

Our model calculations for the month of January (Fig. 3.1a) show that the westward flowing north equatorial current (North East Monsoon Current) in the latitudinal belt (2-6°N) impinges on the Somali coast with one branch flowing towards north-northeast and the other branch flowing southwestwards along the coast as Somali Current. Its magnitude is as high as 80cm/s. The southward flowing winter Somali current meets the northward flowing East African Coastal Current (EACC) at about 5°S, causing a confluence and flows towards east as south Equatorial Counter Current (SECC). The north-northwestward flowing current travels along

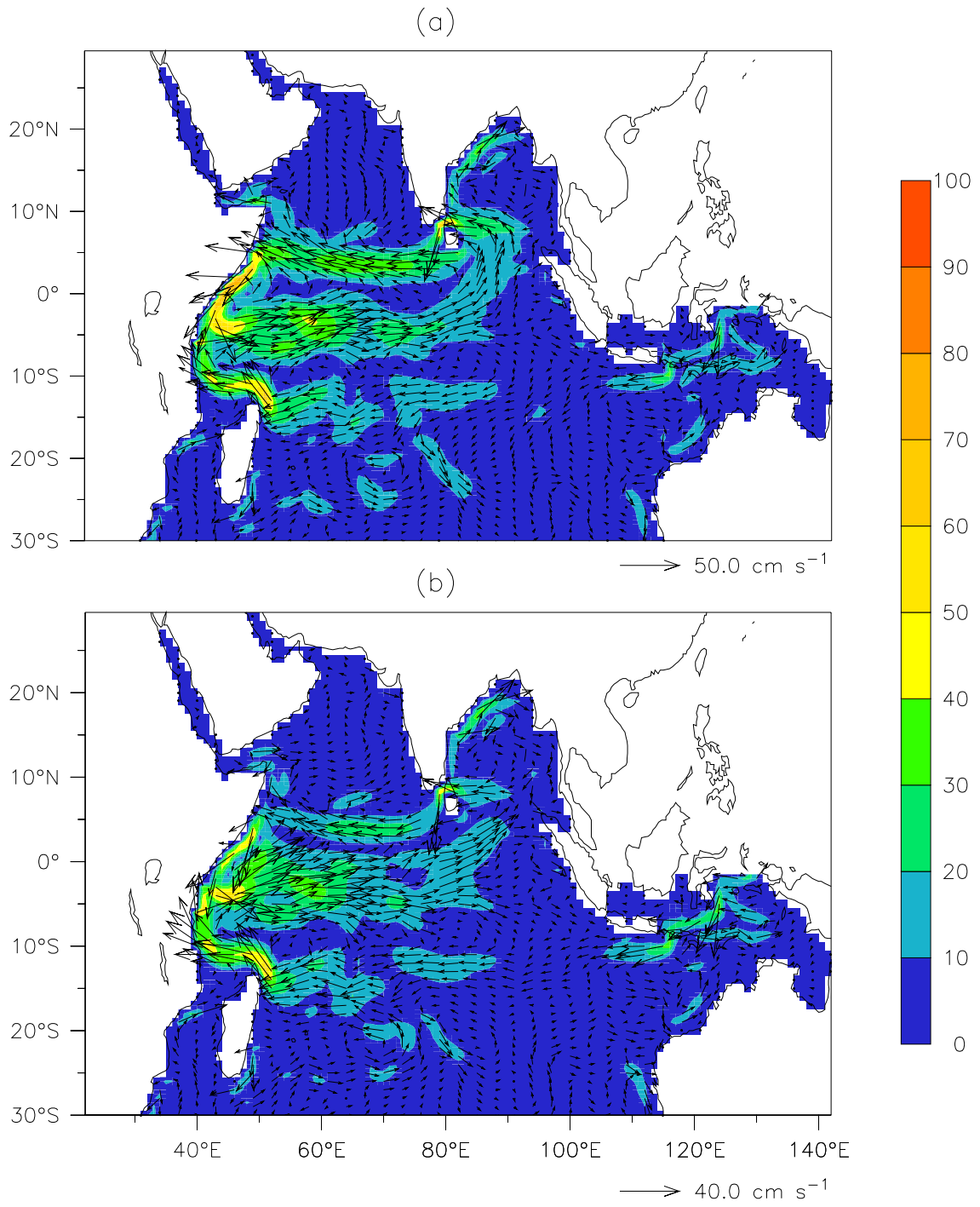


Fig.3.1. Semi diagnostic model velocity (cm/s) for the month of January  
(a) Surface (b) 50 m

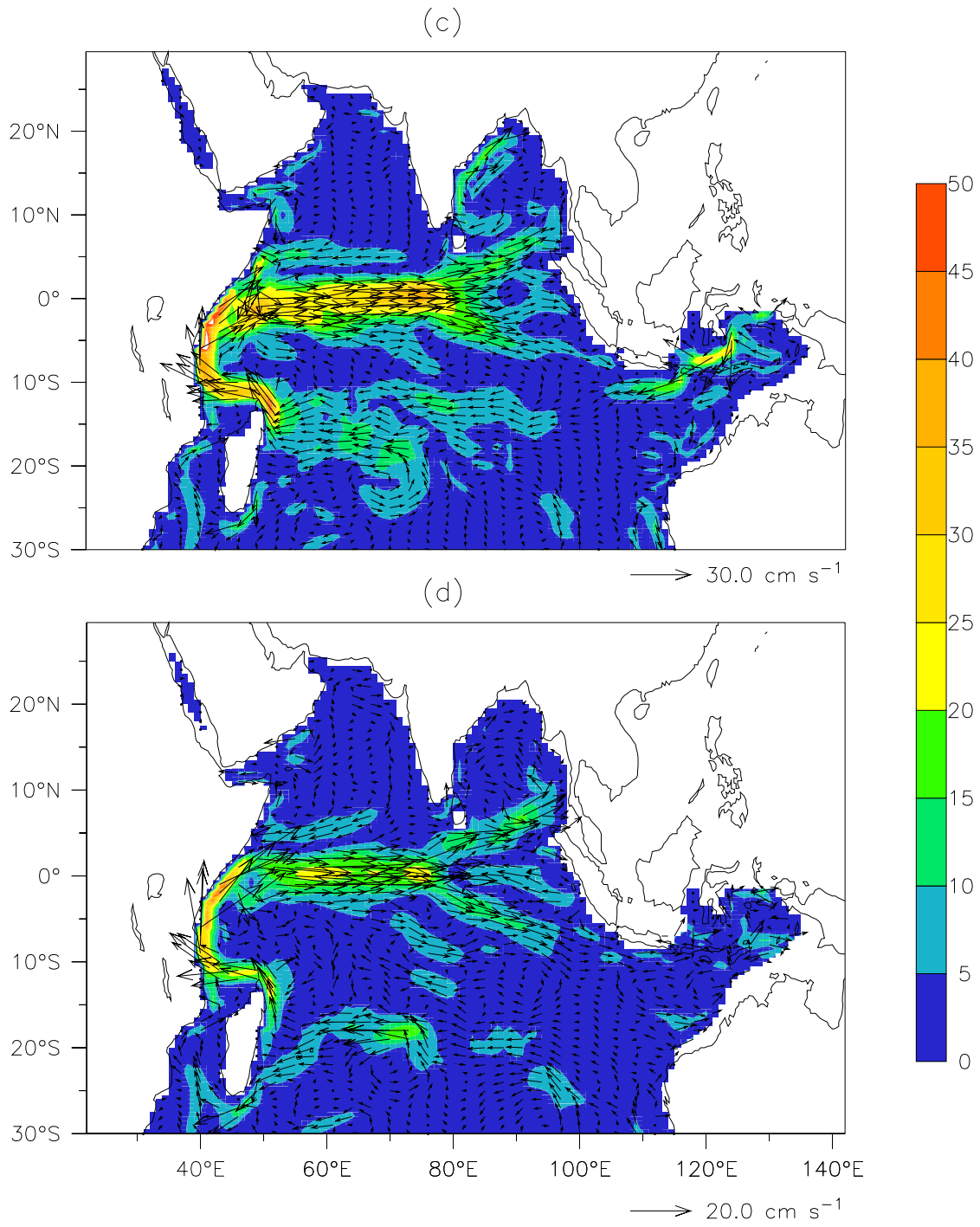


Fig.3.1. continued (c) velocity at 150 m  
(d) velocity at 300 m

the coasts of Arabia and to the northern Arabian Sea as a weak current with a magnitude of  $10\text{-}15\text{ cm s}^{-1}$ . The Socotra eddy could not be reproduced in the model calculation because of its low resolution. Along the west coast of India, a weak current with a magnitude of approximately  $10\text{-}15\text{ cm s}^{-1}$  flows poleward. This current is known as West India Coastal Current (WICC) and it flows poleward against the prevailing weak northerly winds.

The ship drift observations (Cutler and Swallow, 1984) show the presence of northeast monsoon current that flows westwards during January, the southwestward flowing Somali current and the weak West India Coastal Current (Fig. 3.13). Our semi-diagnostic model calculations reproduced very well all the said major currents in the Arabian Sea during the northeast monsoon season.

The computed circulation for 50 m depth (Fig. 3.1b) is almost similar to those observed at the surface, the only difference being that there is a weak eastward flow in the central Arabian Sea between the latitudinal belt  $7^{\circ}\text{N} - 12^{\circ}\text{N}$ . The poleward flowing West India Coastal Current could be seen at 50 m depth also, but its strength is considerably reduced. In the northern Arabian Sea north of  $15^{\circ}\text{N}$ , the flow field is towards north or northeastwards. The strength of the northeast monsoon current is considerably reduced at 50 m. depth. At 150 and 300 m depths, a reversal in the direction of currents as compared to surface current system has been noticed (Fig. 3.1 c-d). There is also development of an equatorward flowing undercurrent along the west coast of India. The northeastward flowing Somali undercurrent is well developed at both these depths.

Model calculations on mean currents at the surface, 50 m, 150 m and 300 m depths for the month of April (intermonsoonal period) are presented in Figs. (3.2 a-d). During the intermonsoonal period, the strength of the wind

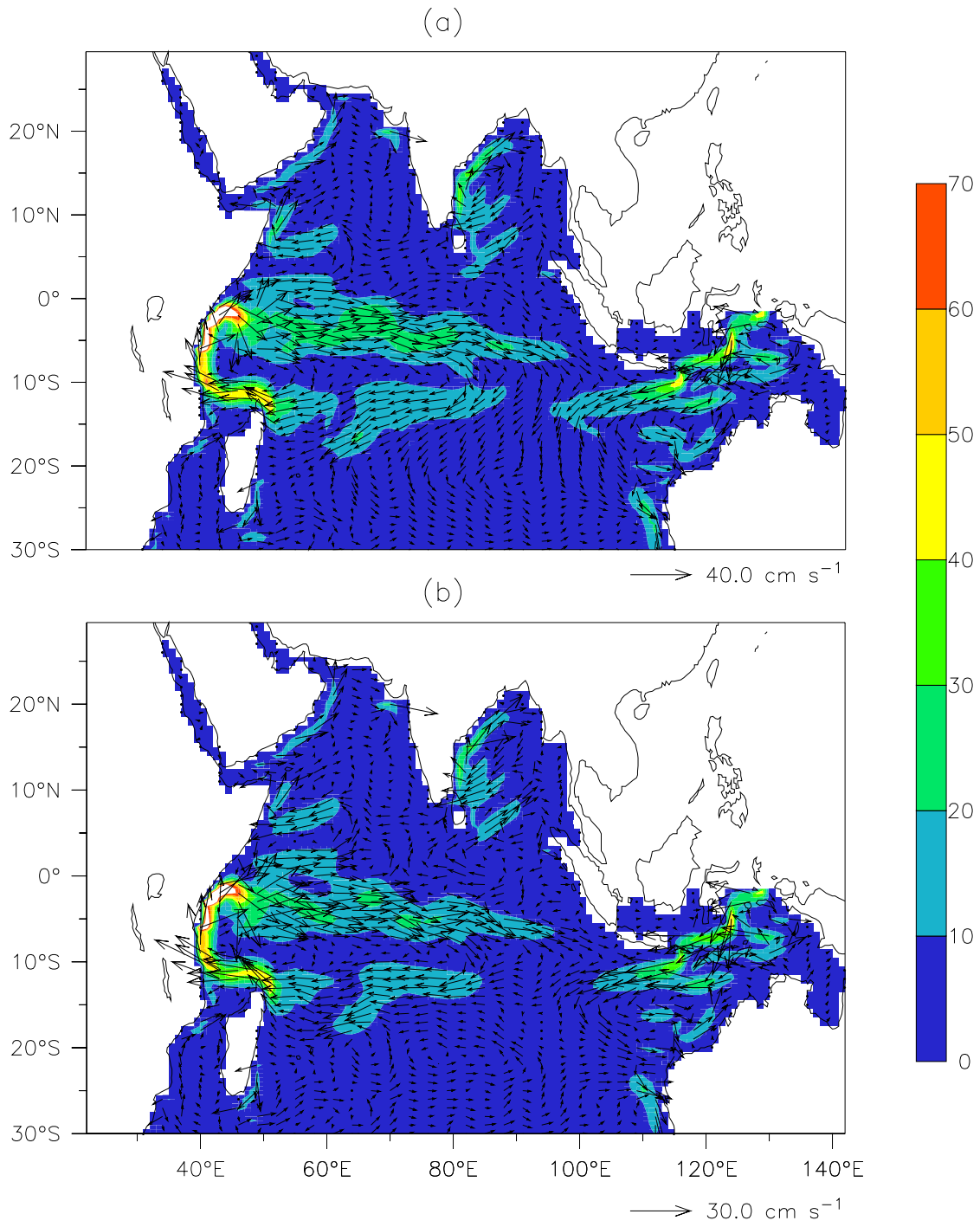


Fig.3.2. Semi diagnostic model velocity (cm/s) for the month of April  
 (a) Surface (b) 50 m

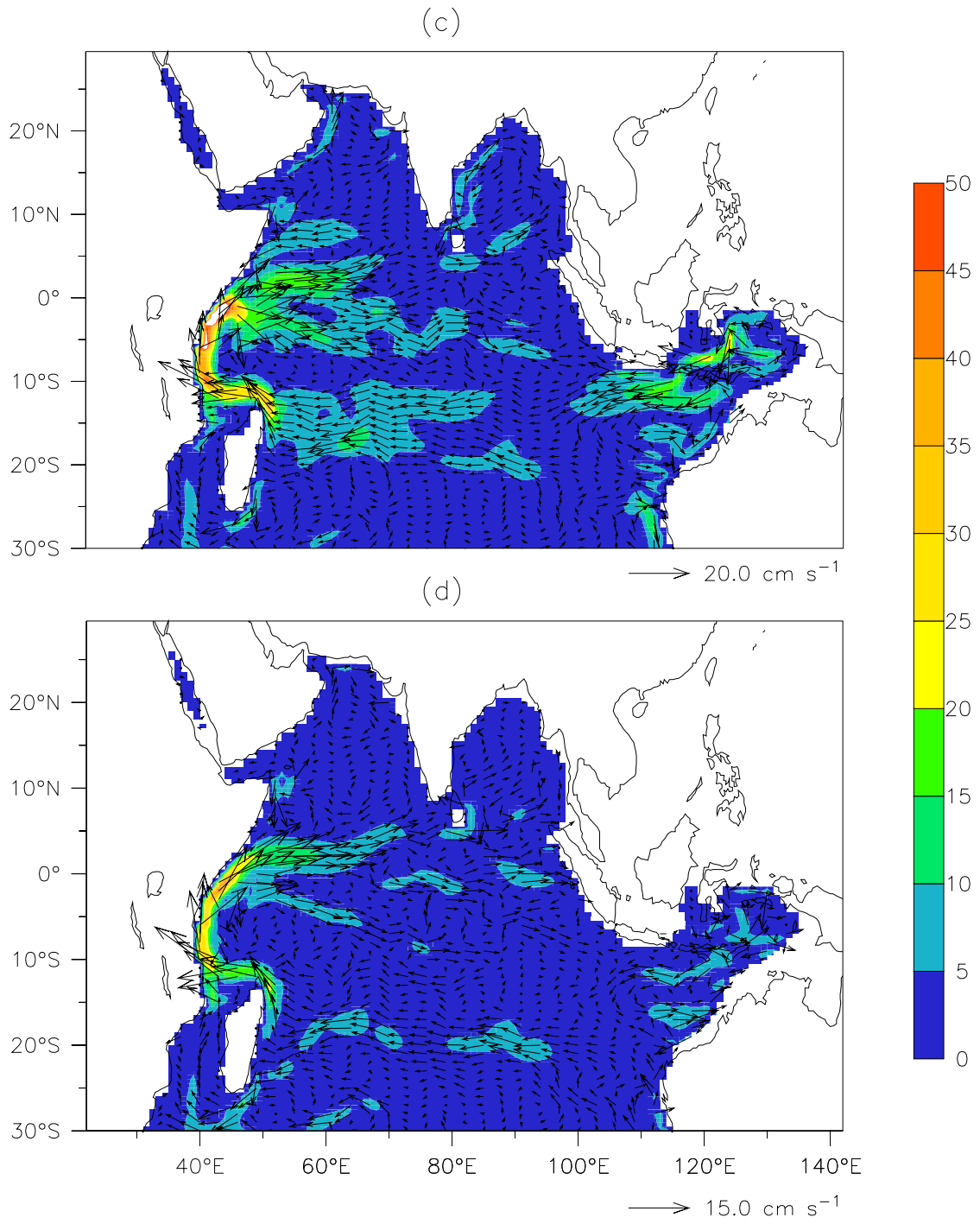


Fig.3.2. continued (c) velocity at 150 m  
(d) velocity at 300 m

field is considerably reduced over the Indian Ocean area. South of 10°S, the southeast trades are present throughout the year. A unique wind forcing pattern over the Indian Ocean area, unlike the other world oceans, is the occurrence of a semi-annual eastward winds over the equator during April. Because of the considerable reduction in the intensity of wind field during the transition season, the flow field is essentially controlled by the internal density field and remote forcings. The westward flowing North East Monsoon Current (NMC), which is a prominent current during the northeast monsoon season, is still present in the latitudinal belt 5°N - 10°N during April, but its intensity is considerably reduced. The westward flowing current within the latitudinal belt 5°N - 10°N turns northward after impinging on the Somali coast at around 5°N, and a fairly strong north-northeastward flow could be seen all along the coasts of Somalia and Arabia. A clear, anticyclonic circulation consistent with the prevailing wind field is noticed in the entire northern Arabian Sea north of 5°N at the surface layers during April. A weak equatorward flowing WICC could be seen all along the west coast of India in April at both the surface and 50 m depths. Ship-drift observations (Cutler and Swallow, 1984) also show weak equatorward WICC along the west coast of India, and these observations are consistent with our model calculations (Fig. 3.14). The computed circulation patterns at 50 m depth during April are almost analogous to what is observed at the surface, but its magnitude is further reduced. A fairly strong northeastward flowing coastal current along the northern Somali and Arabian coasts are still prevalent at 50 m depth. No well organized circulation features could be seen in the northern Arabian Sea at 150 m and 300 m depths during April; however, a well defined southward Somali undercurrent is developed just beneath the northward surface flow at 150 m and 300 m depths.

The computed circulation at the surface for the month of July (Fig. 3.3a) shows the presence of northward flowing Somali current, the Southern Gyre (SG) and the Great Whirl (GW). The southern gyre is central around

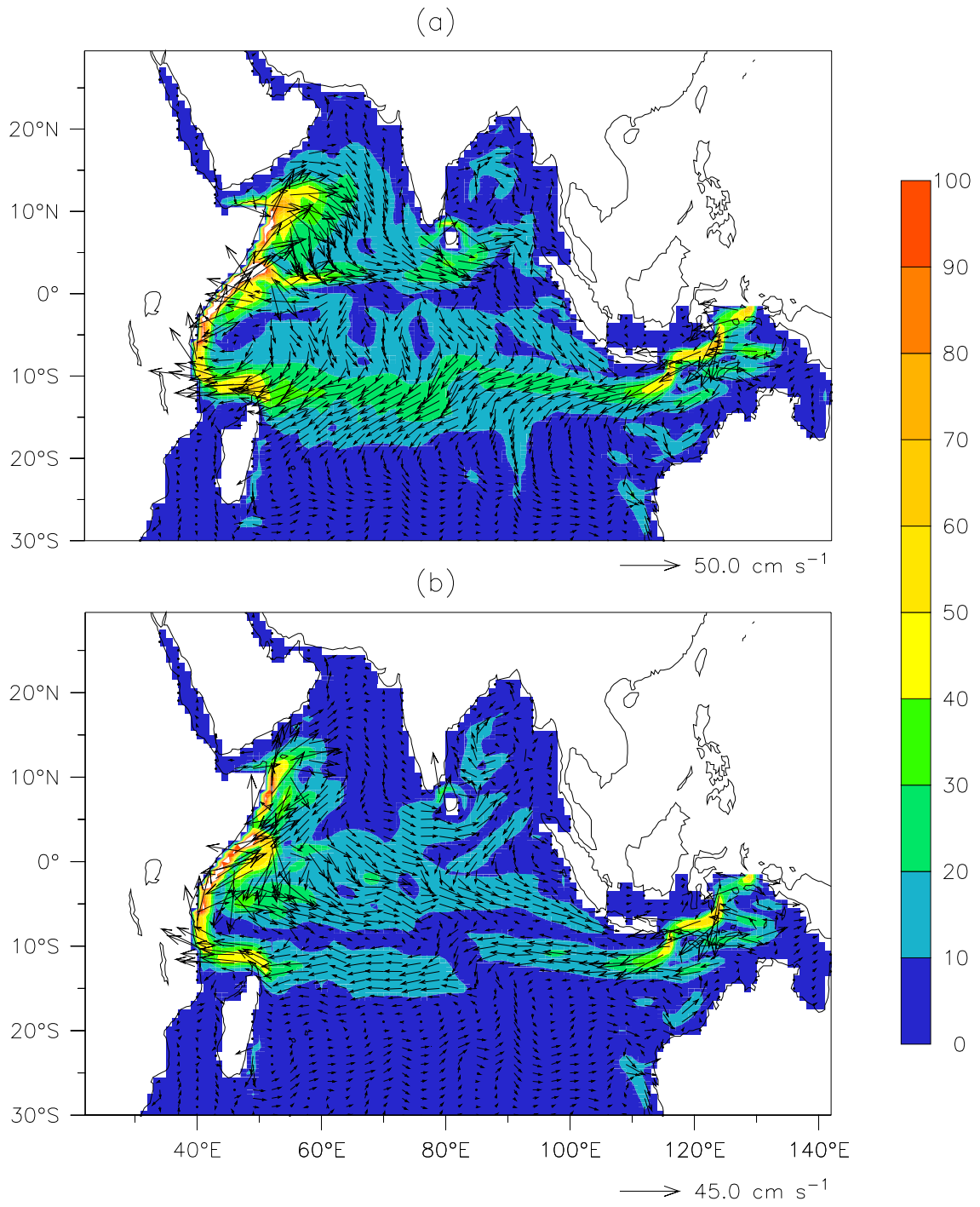


Fig.3.3. Semi diagnostic model velocity (cm/s) for the month of July

(a) Surface (b) 50 m



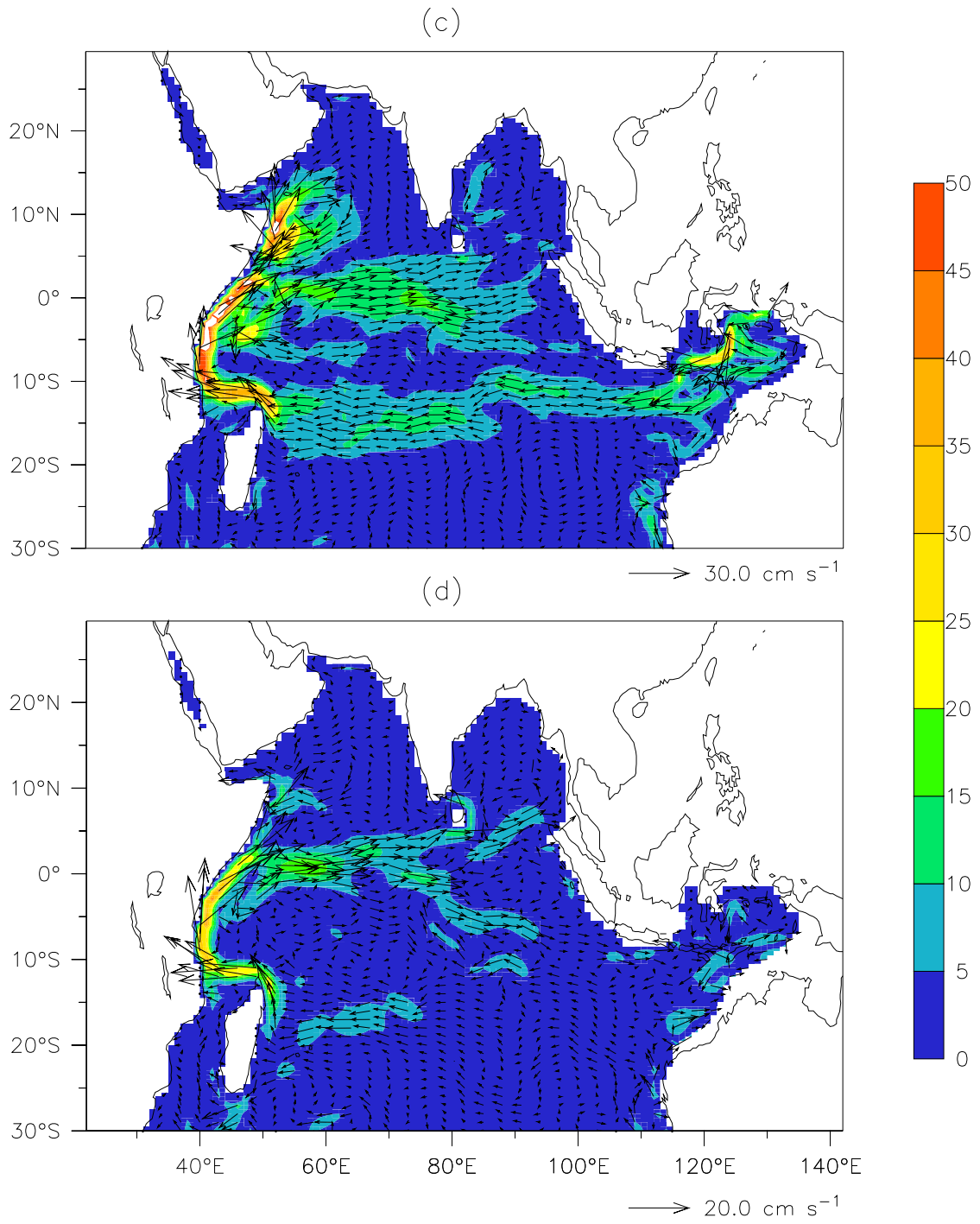


Fig.3.3. continued (c) velocity at 150 m  
(d) velocity at 300 m

5°S and the northern gyre is centred around 7°N latitude. The surface circulation pattern shows the presence of SC as an extension of the East African Coastal Current (EACC) that flows northward across the equator to about 3-4°N with a magnitude of approximately 100 cm s<sup>-1</sup>. At 4°N, the Somali current partially turns eastward and partially flows back across the equator in a circulation pattern referred to as “Southern Gyre”. The Great Whirl (GW) develops from 4°N to 12°N where it turns offshore. In the semi-diagnostic calculations, only the local forcings of wind stress and the internal density fields were considered, and it reproduced fully the gyres in the Somali current system during the summer season. It can be inferred that the Somali current system is mainly forced by the alongshore wind associated with the Findlater Jet, its offshore weakening that produces a region of strong negative wind stress curl and the internal density field. During the southwest monsoon season, the southwest monsoon current (SMC) flows eastward from June to September. In the model calculations, the SMC flows towards the east with a magnitude of 40 cm s<sup>-1</sup> in the eastern Arabian Sea. The winds during the summer in the northern Arabian Sea are southwesterly and this wind would induce an Ekman drift current directed south of east. Primarily, the SMC is wind-driven, although the influence of density gradient on the strength and direction of flow could be seen to a certain extent. McCreary et al. (1993) and Vinayachandran (1999a) attributed two driving mechanisms for the SMC; one is the local forcing by the wind and the other is the remote forcing effect which accounts for the northward bending of SMC into the Bay of Bengal. The west India coastal current flows equatorward along the west coast of India with a magnitude of approximately 20-30 cm s<sup>-1</sup> during summer. Our model calculations reproduced well the characteristics of SMC during the summer season and hence it is inferred that the SMC is driven by local forcings.

The model calculation of currents at 50m, 150m and 300m depths during the southwest monsoon season are presented in Fig. 3.3 (b-d). The

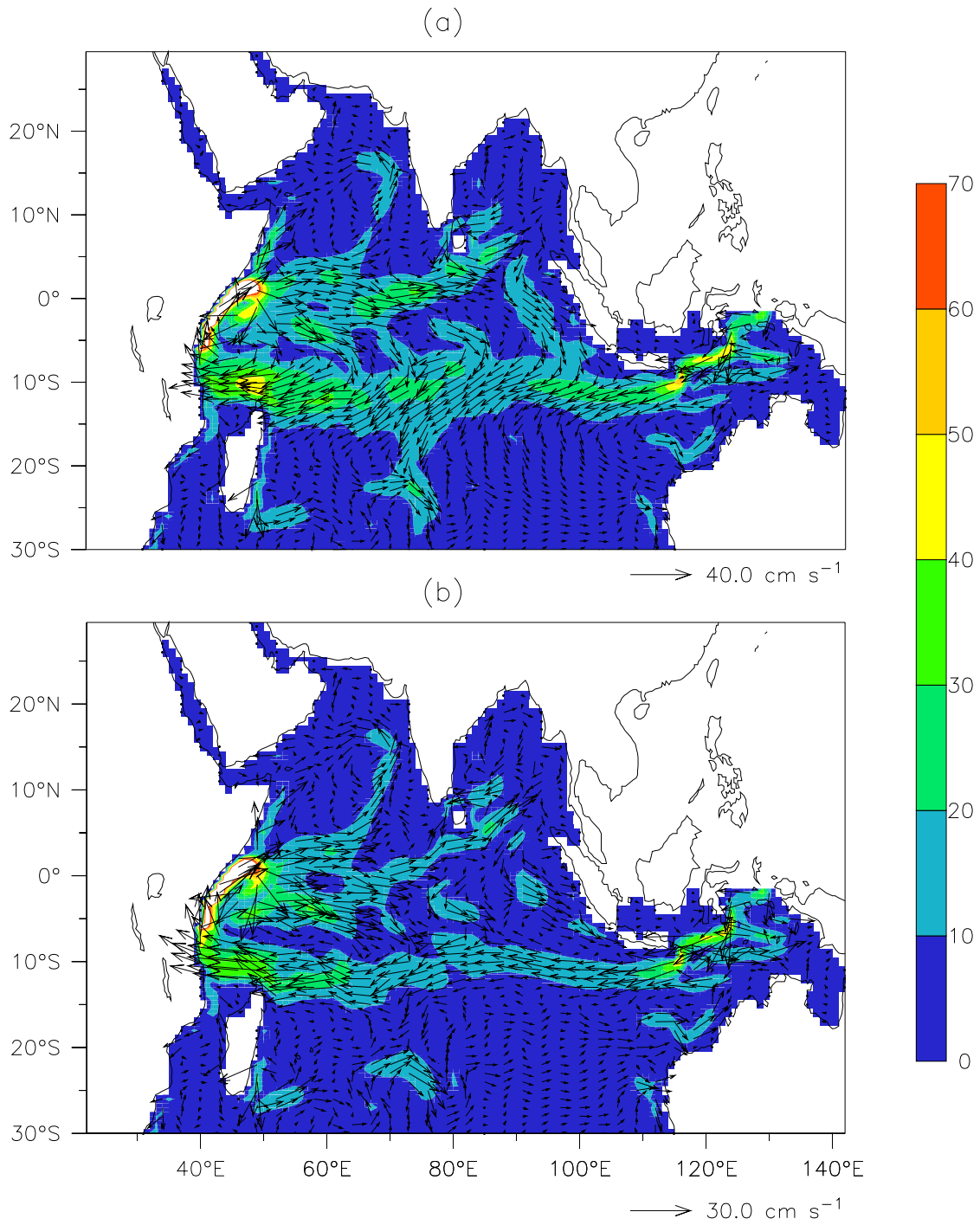


Fig.3.4. Semi diagnostic model velocity (cm/s) for the month of October  
 (a) Surface (b) 50 m

strength of WICC that flows along the west coast of India is decreased at 50 m depth. In the west, off the coast of Somalia, the great whirl and the southern gyre (SG) observed during the southwest monsoon period at the surface are still present at 50 m depth. The strength of SMC was reduced to  $25 \text{ cm s}^{-1}$  at 50 m depth. There is also development of an equatorward flowing undercurrent along the west coast of India at 150 m and 300 m depths. (Fig.3.3 c-d). The northeastward flowing summer Somali current, the two clockwise gyres and SMC are still present at 150 m and 300 m depths. The mean current pattern at 300 m depth is almost analogous to what is observed at 150 m depth, the only difference being that the overall magnitude of current is further reduced at this depth.

During the month of October, the northeastward flowing Somali current observed during the southwest monsoon season is still present all along the Somali coasts at the surface and 50 m depths. In addition, a clockwise eddy with a diameter of approximately 500 kms is formed near the Somali coasts between  $5^{\circ}\text{S}$  and  $5^{\circ}\text{N}$  latitudes. These results are in full agreement with shipdrift observations (Cutler and Swallow, 1984). Model results show a southward Somali undercurrent beneath the northward flowing summer surface Somali current. This southward Somali undercurrent could be seen both at 150 m and 300 m depths (Figs. 3.4 c-d). Another important observation during October is that a clear cyclonic circulation which could be seen both at the surface and 50 m depths, is developed in the Central Arabian Sea. A weak northward WICC is found at the surface and 50 m depth along the west coast of India.

#### **3.4.2 Spatial variability of monthly mean currents in the upper layers of the Bay of Bengal**

The winds over the Bay of Bengal are southwesterly during May-September and northeasterly during November-January. The transition from southwest to northeast takes place during February. Though, these winds are strongest during the monsoons, the ocean circulation is best

developed during the transition season from February to April. However, there are minor variations in the wind stress field pattern during different months within a particular season. It is noted that the northern and Eastern Bay of Bengal is under the influence of northerly winds during the month of January. The wind stress curl fields also change in correspondence to seasonal wind stress reversals. Over the western Bay of Bengal, the curl is cyclonic in summer (July) and anticyclonic in winter.

During the transitions months of April and October, the wind field is generally weak over the entire Bay of Bengal. During April, southerly and southwesterly winds prevail over the western and northern Bay of Bengal, whereas weak westerly winds are observed in the central and eastern Bay of Bengal. In October, fairly strong westerly and southerly winds could be seen off the coast of Sri Lanka, while weak cyclonic type of wind circulation is observed in the entire central and northern Bay of Bengal (Fig. 2d). It is observed that the western Bay of Bengal is subjected to strong seasonal reversals of wind stress forcing. As a result, the processes that influence EICC are similar to those that affect the Somali current system. Because the local winds are weaker, the effects due to remote forcing are relatively more significant for the Bay of Bengal than they are for the Arabian Sea.

The seasonal cycle of EICC and the Bay of Bengal circulation has been investigated from analysis of ship-drift currents and shipboard surveys by Shetye et al. (1991a,b; 1993; 1996) and more recently by Vinayachandran and Yamagata (1998). During January, at the peak of the winter monsoon, the southward EICC decreases in strength and north of 15°N even reverses direction. From March to May, poleward flowing EICC strengthens, even though the local winds are very weak.

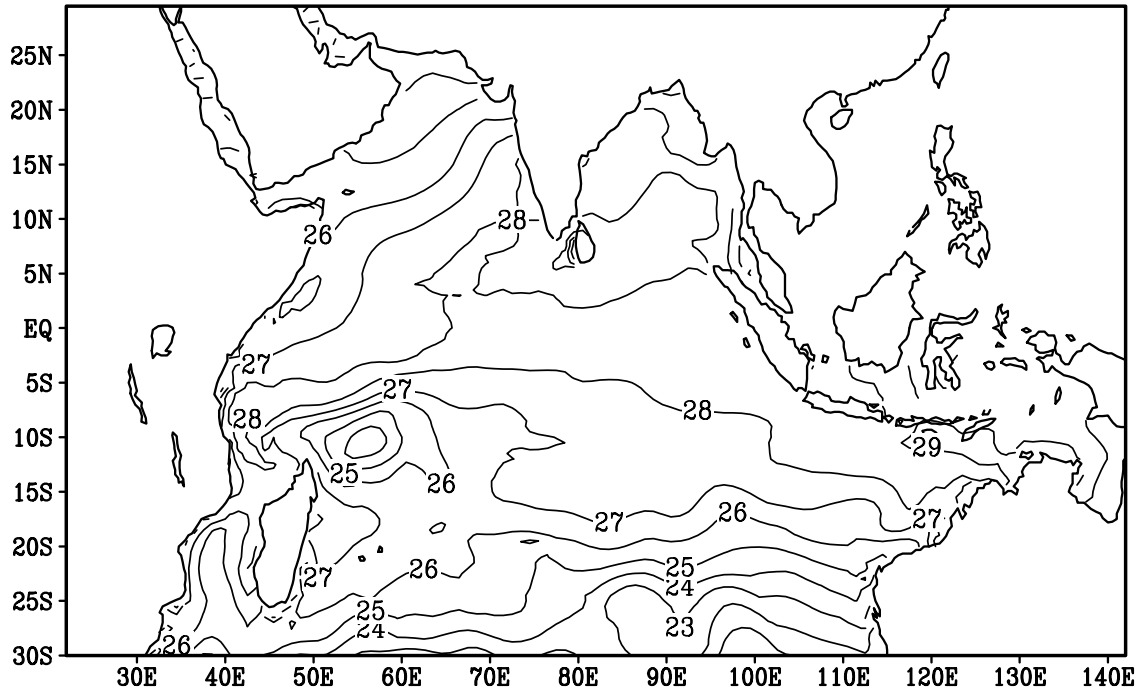
With the onset of summer monsoon, the northward EICC weakens and a southward current appears off the eastern Srilanka. Using shipdrift currents and surface geostrophic flows derived from T/P, Eigenheir and

Quadfasel (2000) showed that, at the height of summer monsoon, there is a western boundary confluence near 10°N, with the EICC flowing northward to the north of 10°N and southward south of it. According to Vinayachandran et al. (1999a), the confluence is supplied mostly by SMC across 6°N that circulates cyclonically about a dome of low Sea Surface Height Anomaly (SSHA). By October-November, the shipdrift current shows southward flow everywhere along the east coast of India and Srilanka. At this time, T/P altimetry suggest a slow cyclonic circulation around the Bay of Bengal which breaks up into several cells as the northeast monsoon develops.

The computed mean currents at the surface for the month of January (Fig. 3.1a) show that a large anticyclonic gyre is formed in the entire Bay of Bengal north of 8°N. The East India Coastal Current (EICC) associated with the wind-driven anticyclonic gyre in the Bay of Bengal flows poleward all along the east coast of India from approximately 8°N with a magnitude varying between 20 and 30cm/s. Off the coasts of Myanmar, Eastern Bay of Bengal and Andaman Sea, the flow field is towards south and southwest in response to prevailing westerly winds. The same circulation pattern could be seen at 50 m depth also, but the magnitude of currents is decreased. The EICC that flows poleward at the surface and 50 m depth could be seen at 150 m depth also (Fig. 3.1c); however, the circulation pattern at 150 m depth is completely different from what is observed at the upper layers; a cyclonic gyre was observed at 300 m depth. The model computed mean currents at the upper layers of Bay of Bengal agree with shipdrift observations (Cutler and Swallow, 1984).

To understand the forcing mechanisms of currents in the upper layers of Bay of Bengal, the local forcing parameters of wind stress, temperature and salinity data over the model area were analysed. The temperature and salinity data at the surface and 150 m depth (Levitus, 1994) are presented in Figs. 3.5(1-b) and 3.6(a-b). It is found that the central Bay of

(a)



(b)

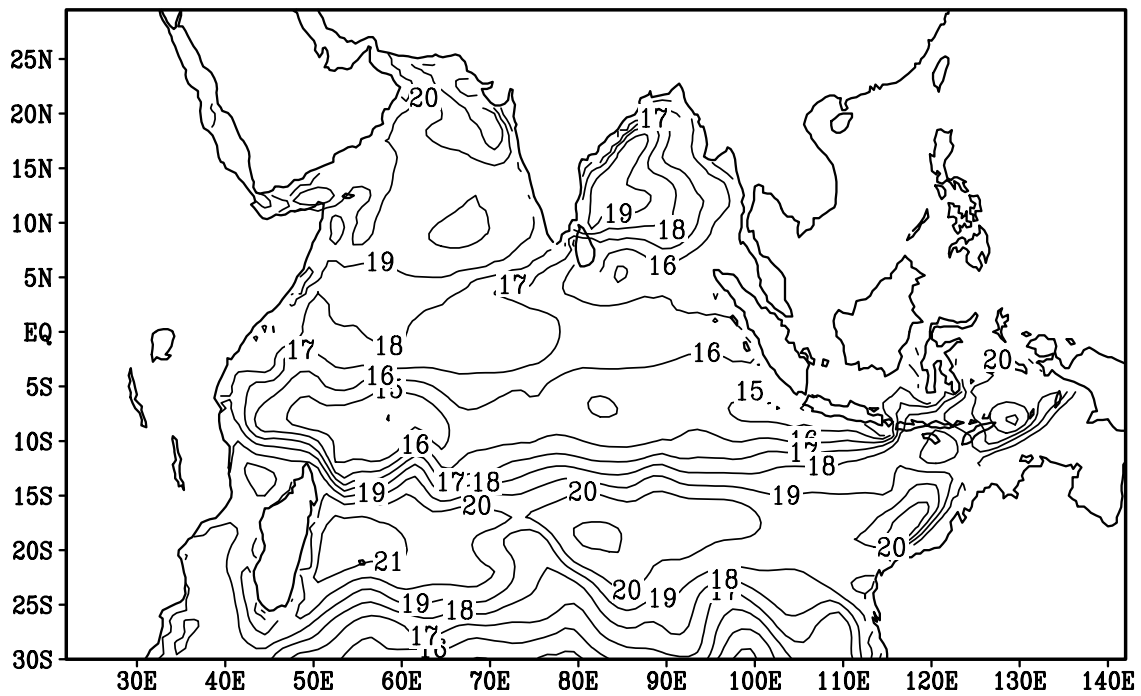
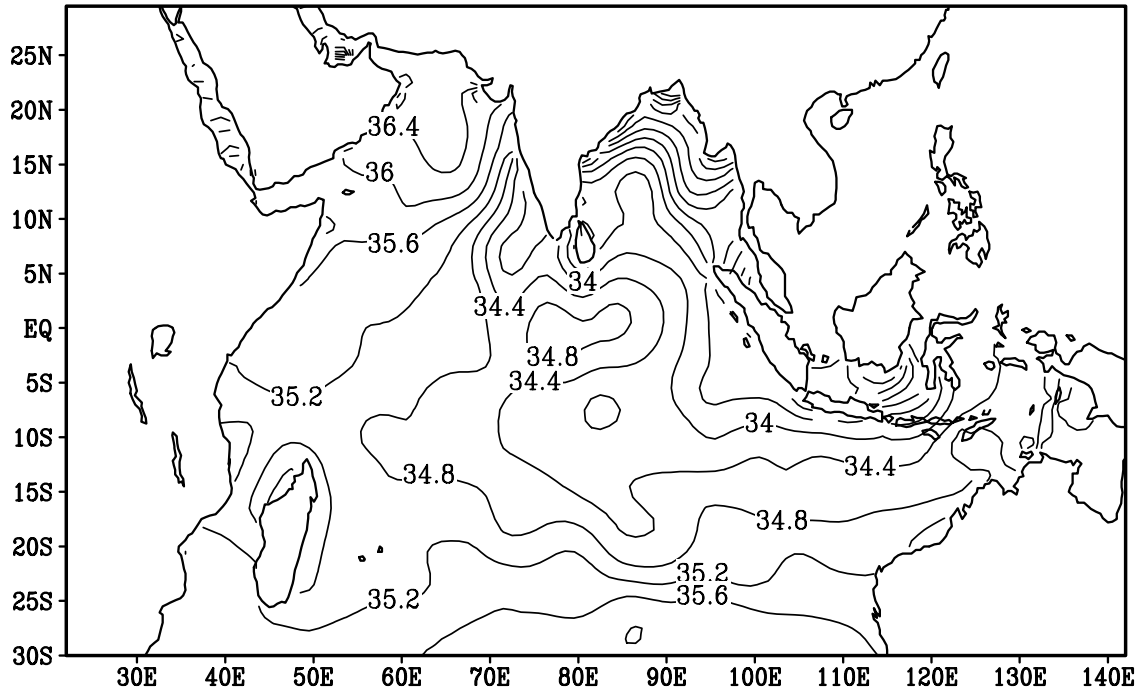


Fig.3.5. Semi diagnostic model temperature (deg C) for January

(a) Surface (b) 150 m

(a)



(b)

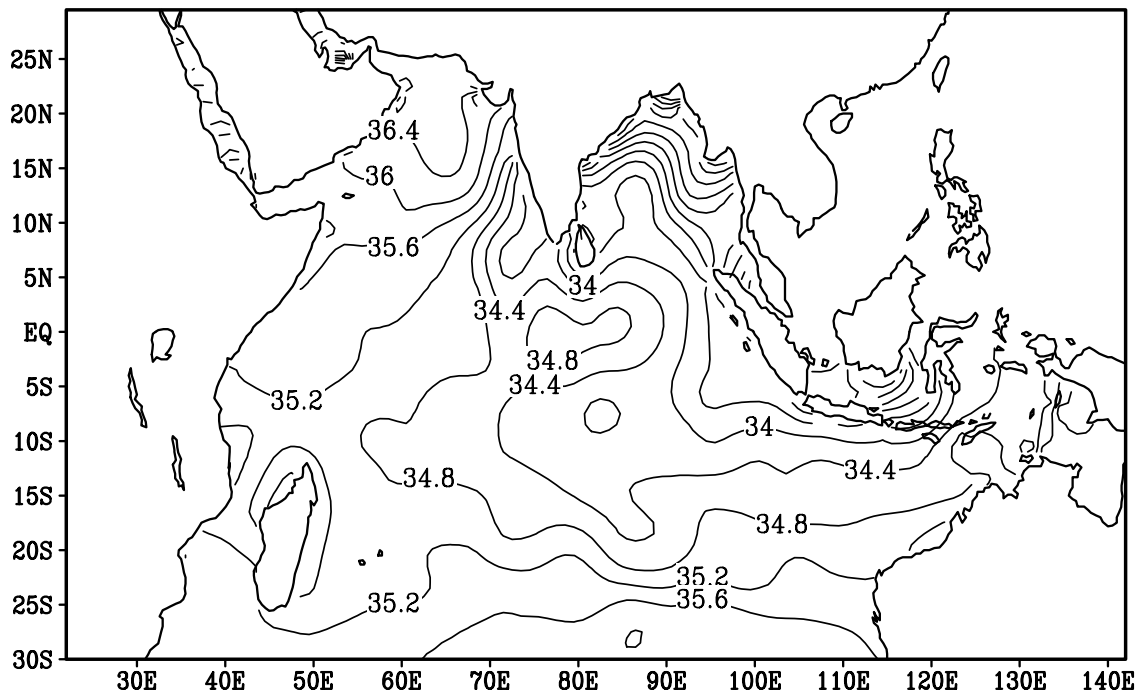


Fig.3.6. Semi diagnostic model salinity (ppt) for January

(a) Surface (b) 150 m

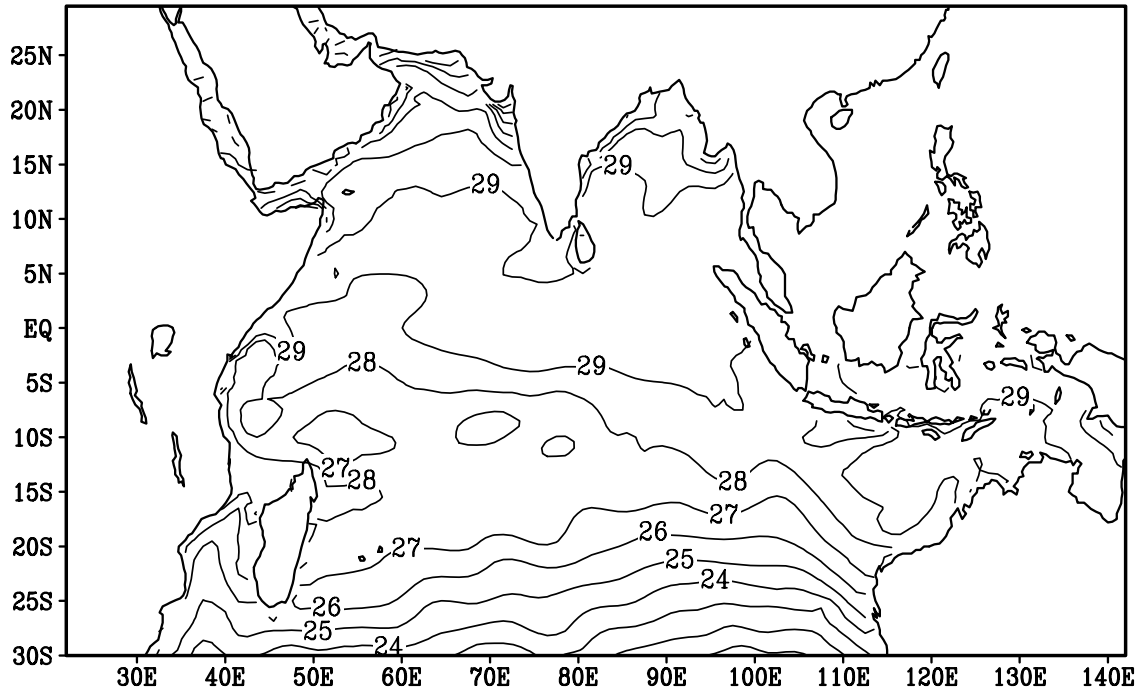


Bengal is characterized by higher temperature compared to coastal regions and such a thermal structure can generate an anticyclonic gyre in the entire Bay of Bengal. The combined effect of local wind forcing and the thermal structure are responsible for the observed circulation pattern in the Bay of Bengal during January. The observed cyclonic circulation at 300 m is not matching with the earlier studies on EICC and bay circulation. Shankar et al., (1996) reported the vertical structure of EICC extending to greater depths and hence the anticyclonic gyre with EICC as the western boundary current will be present at 300 m. The observed cyclonic gyre may be due to the inability of the semi-diagnostic model to reproduce circulation at greater depth due to the lack of long term integrations required to evolve the circulation at deeper levels.

During the month of April, the wind field is very weak over the entire Bay of Bengal, and southerly and southwesterly winds prevail all along the east coast of India. In response to the prevailing southerly wind stress forcing, the EICC flows poleward all along the East coast of India. The model computed EICC fully match with the shipdrift data. The shipdrift data suggest that the wind-driven EICC is part of an anticyclonic gyre formed in the Bay of Bengal during January-May and is best developed during April. This anticyclonic gyre type of circulation could be seen at 50 and 150 depths also, but with a lesser density. There is no organized circulation pattern at 300 m depth. It is suggested that the EICC is the western boundary current of the seasonal anticyclonic gyre that flows in response to negative wind stress curl and warm temperature field prevalent in the central Bay of Bengal (Fig. 3.7a). Even the salinity distribution at the surface (Fig. 3.8a) is highly favourable for the formation of a strong poleward flowing EICC during April.

During the month of July (summer season), the wind field is westerly and southwesterly throughout the Bay of Bengal, and the EICC does not flow poleward in the direction of the wind as expected. Model results show that

(a)



(b)

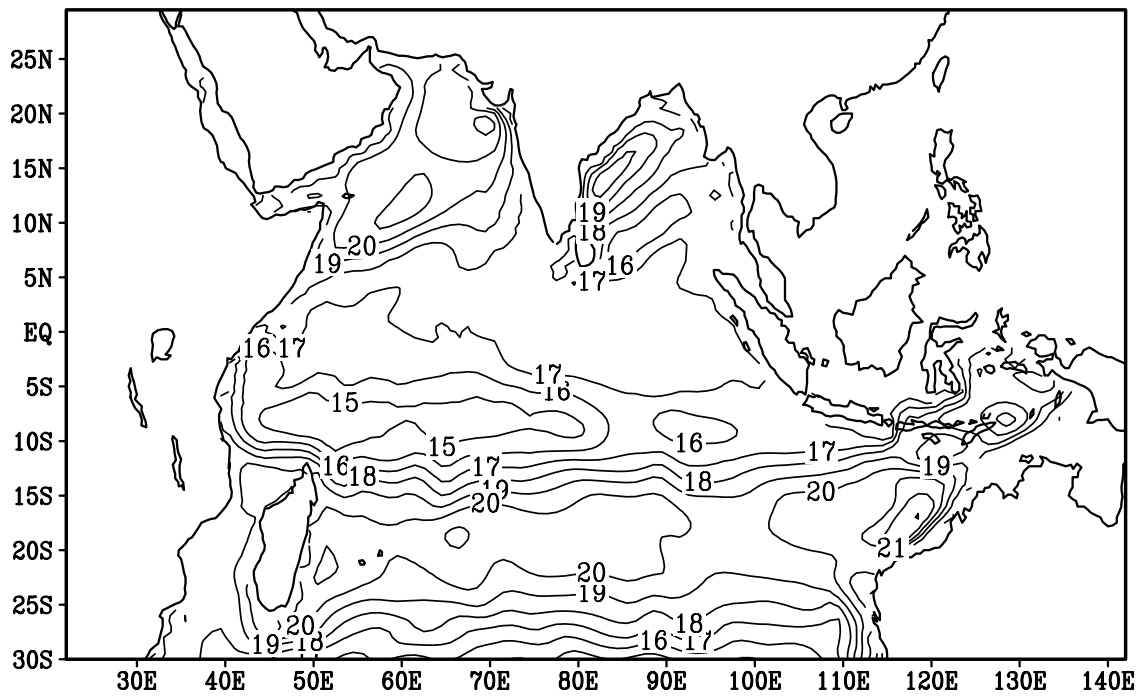
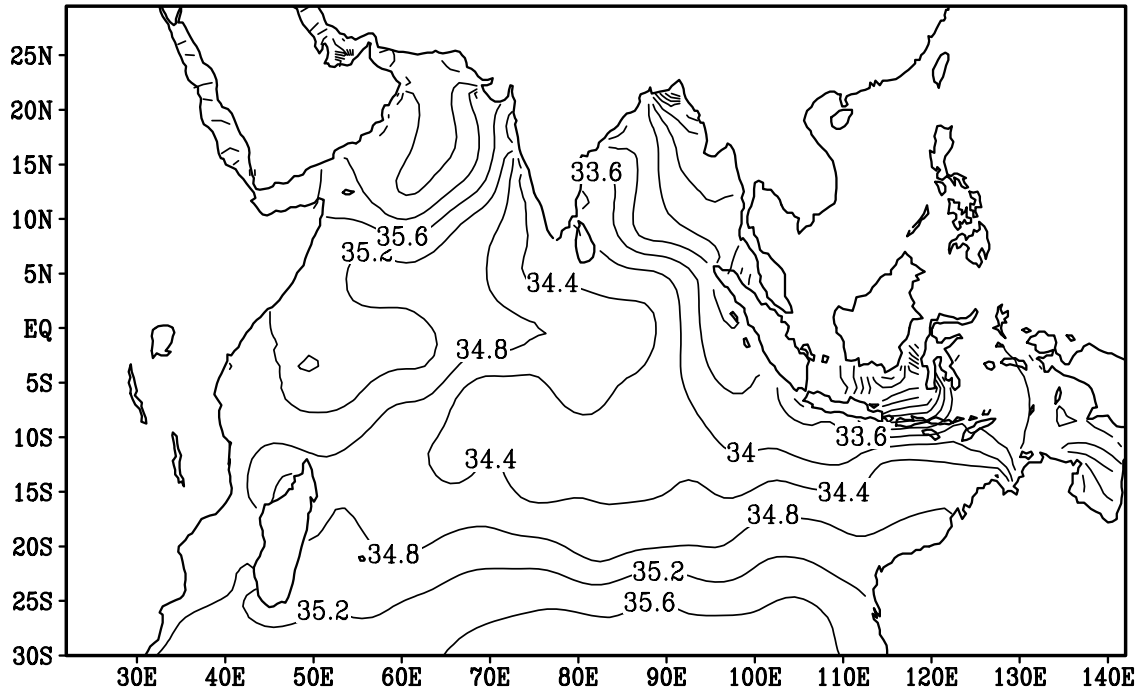


Fig.3.7. Semi diagnostic model temperature (deg C) for April

(a) Surface (b) 150 m

(a)



(b)

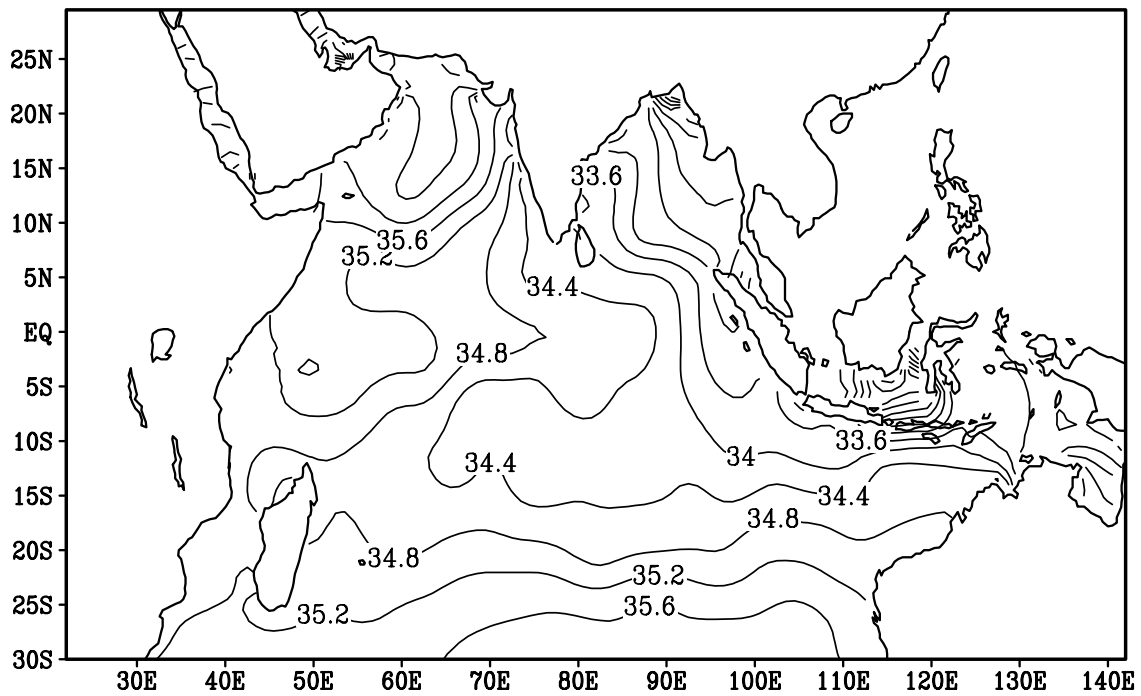
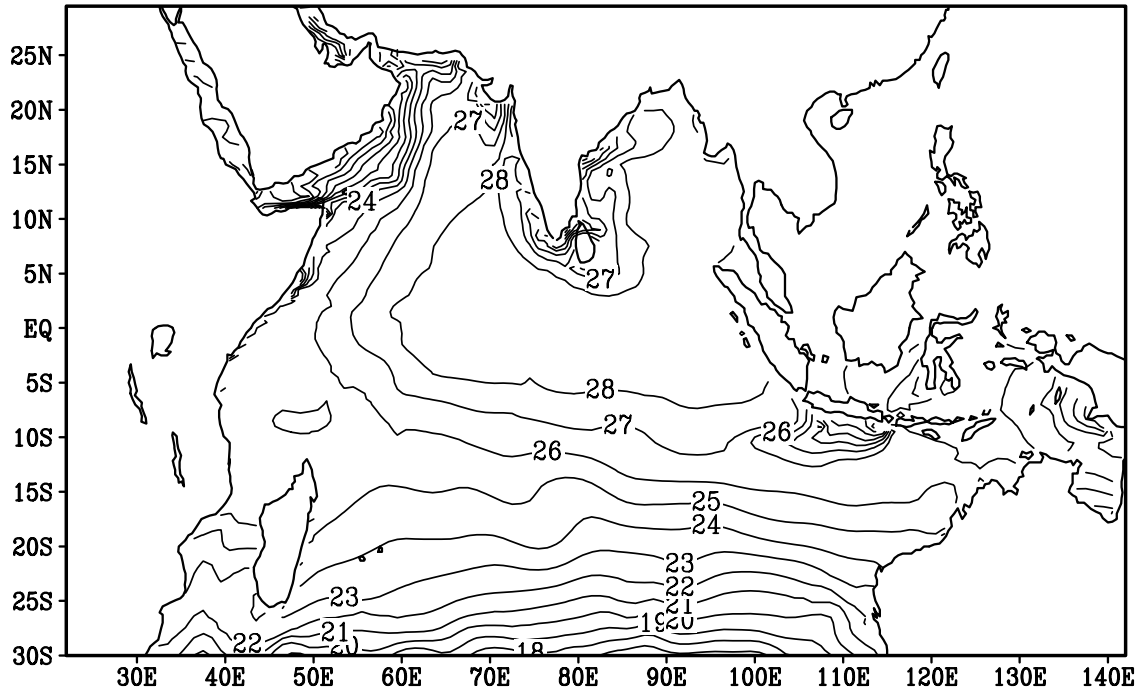


Fig.3.8. Semi diagnostic model salinity (ppt) for April

(a) Surface (b) 150 m

(a)



(b)

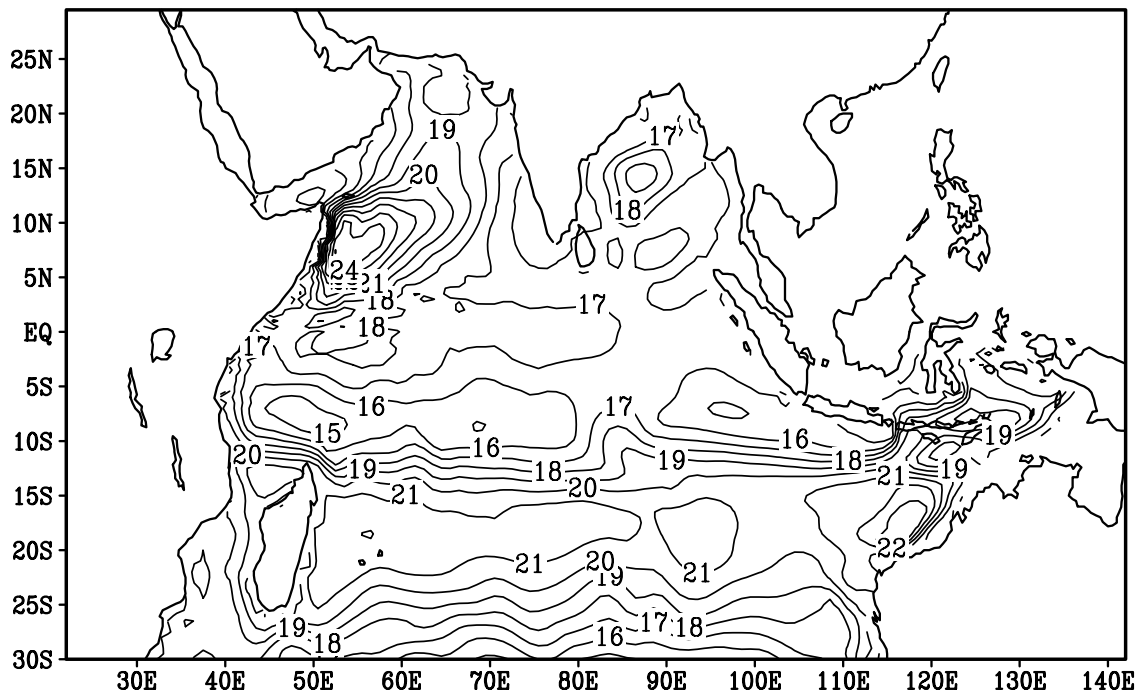
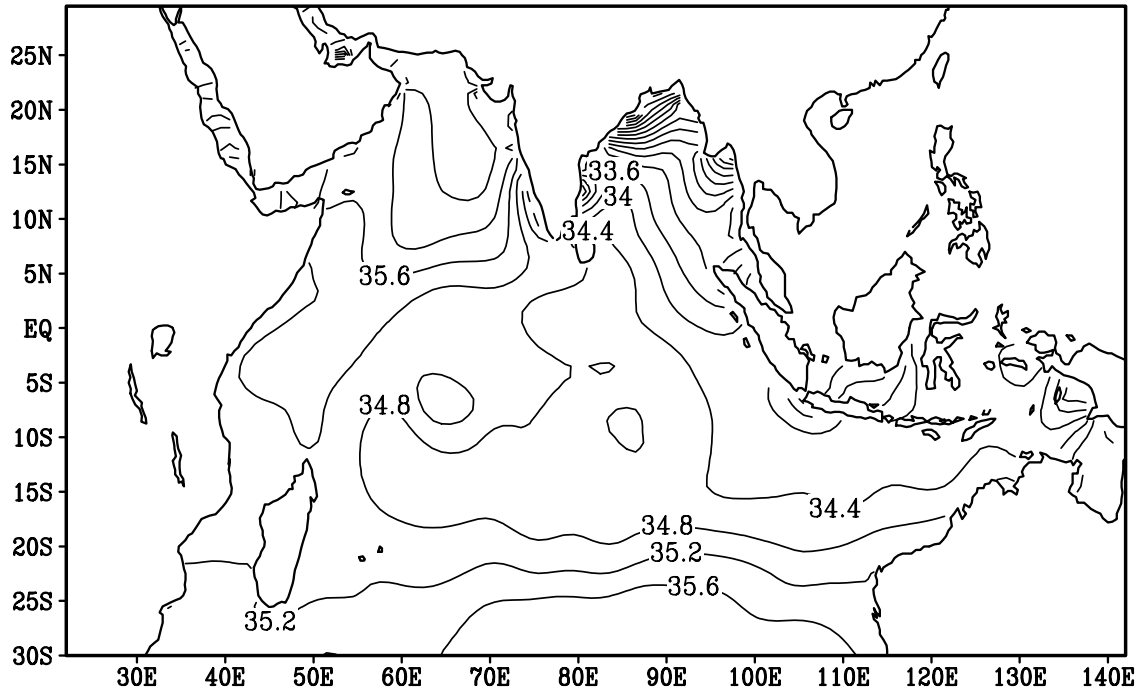


Fig.3.9. Semi diagnostic model temperature (deg C) for July

(a) Surface (b) 150 m

(a)



(b)

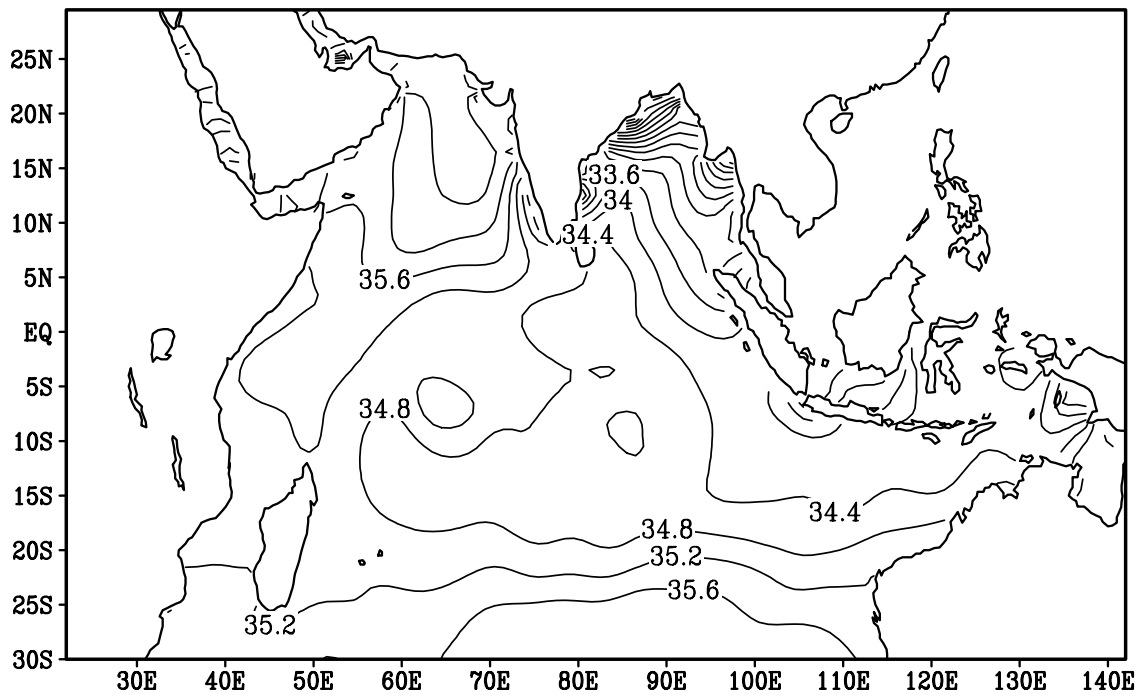
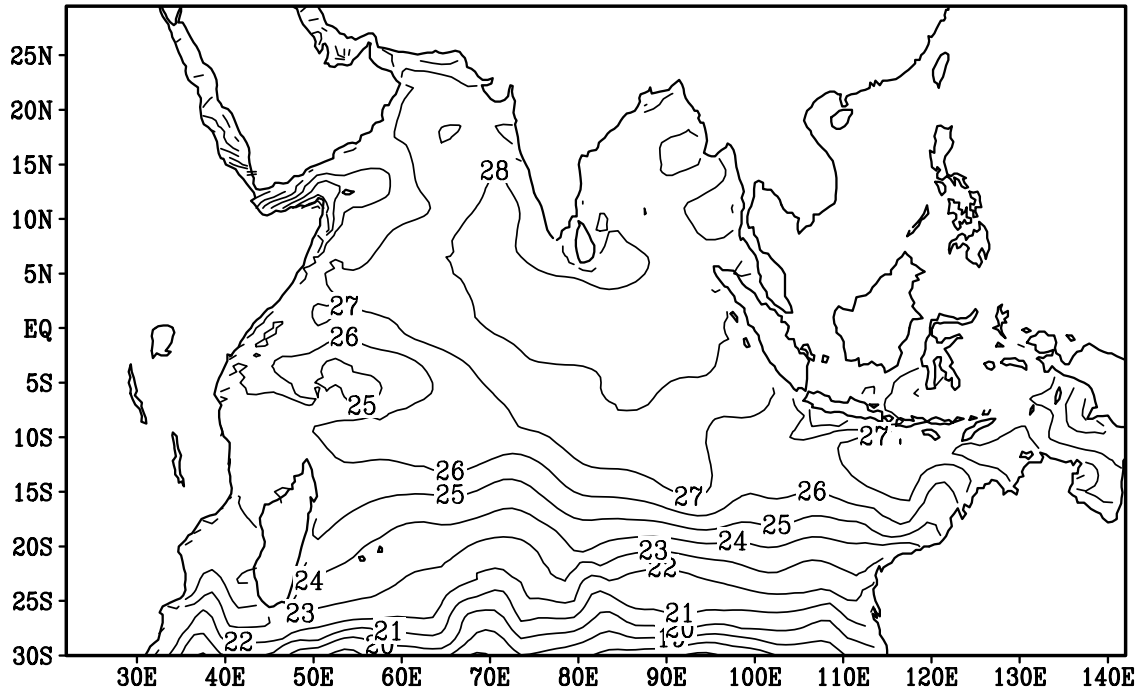


Fig.3.10. Semi diagnostic model salinity (ppt) for July

(a) Surface (b) 150 m

(a)



(b)

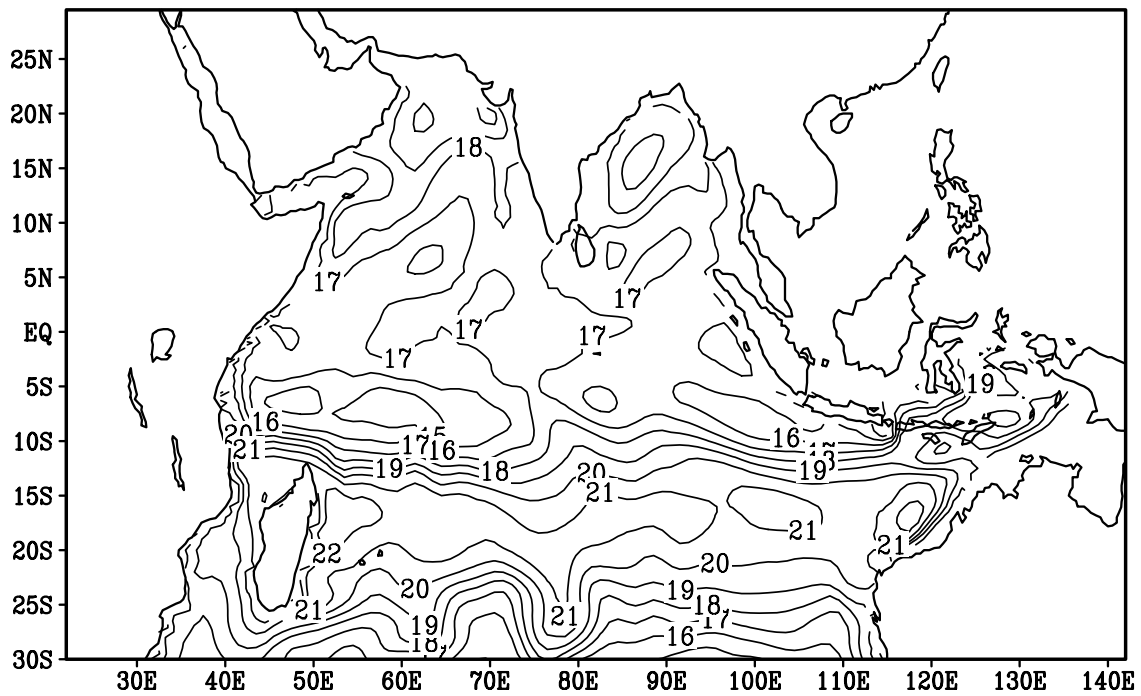
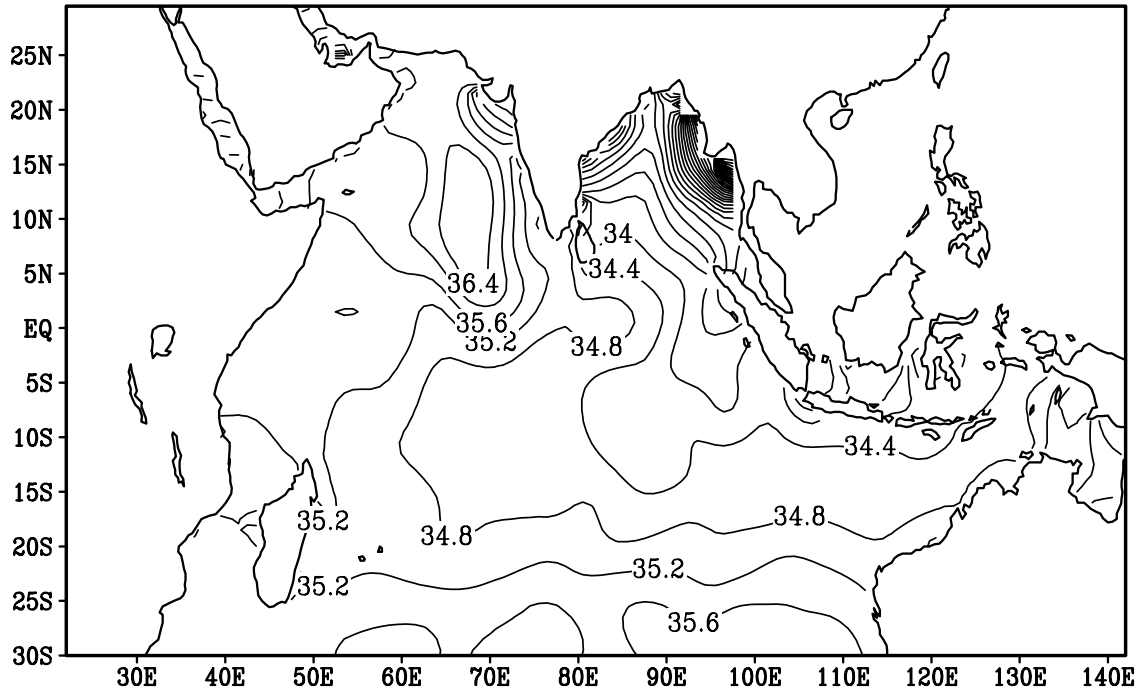


Fig.3.11. Semi diagnostic model temperature (deg C) for October

(a) Surface (b) 150 m

(a)



(b)

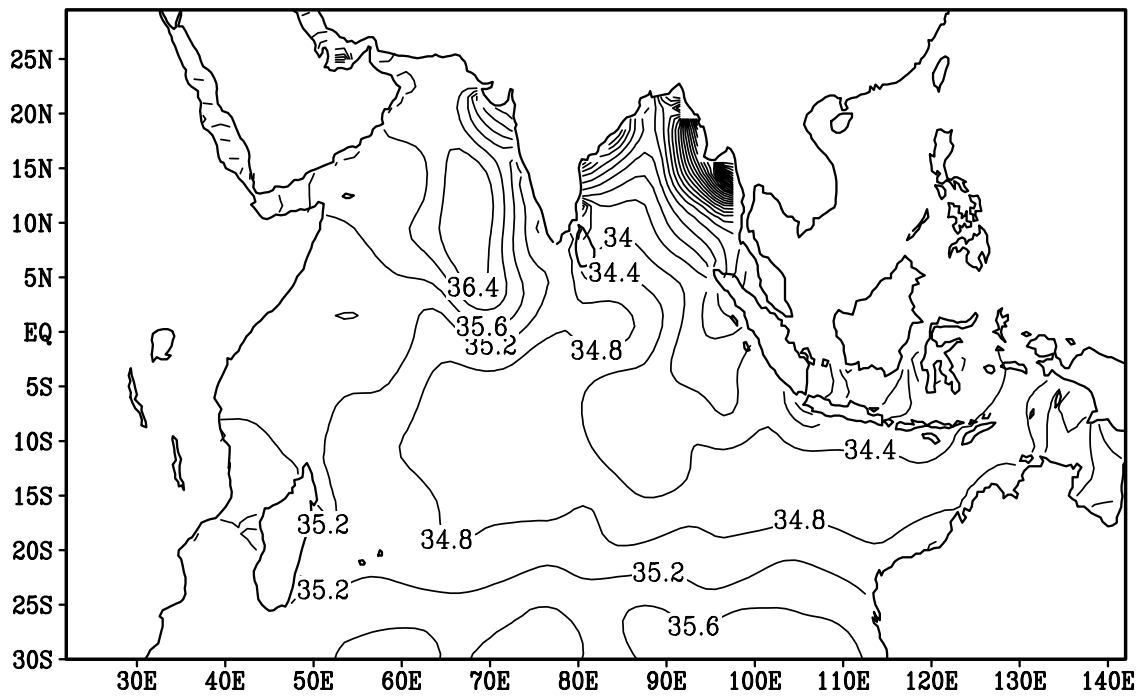


Fig.3.12. Semi diagnostic model salinity (ppt) for October  
(a) Surface (b) 150 m

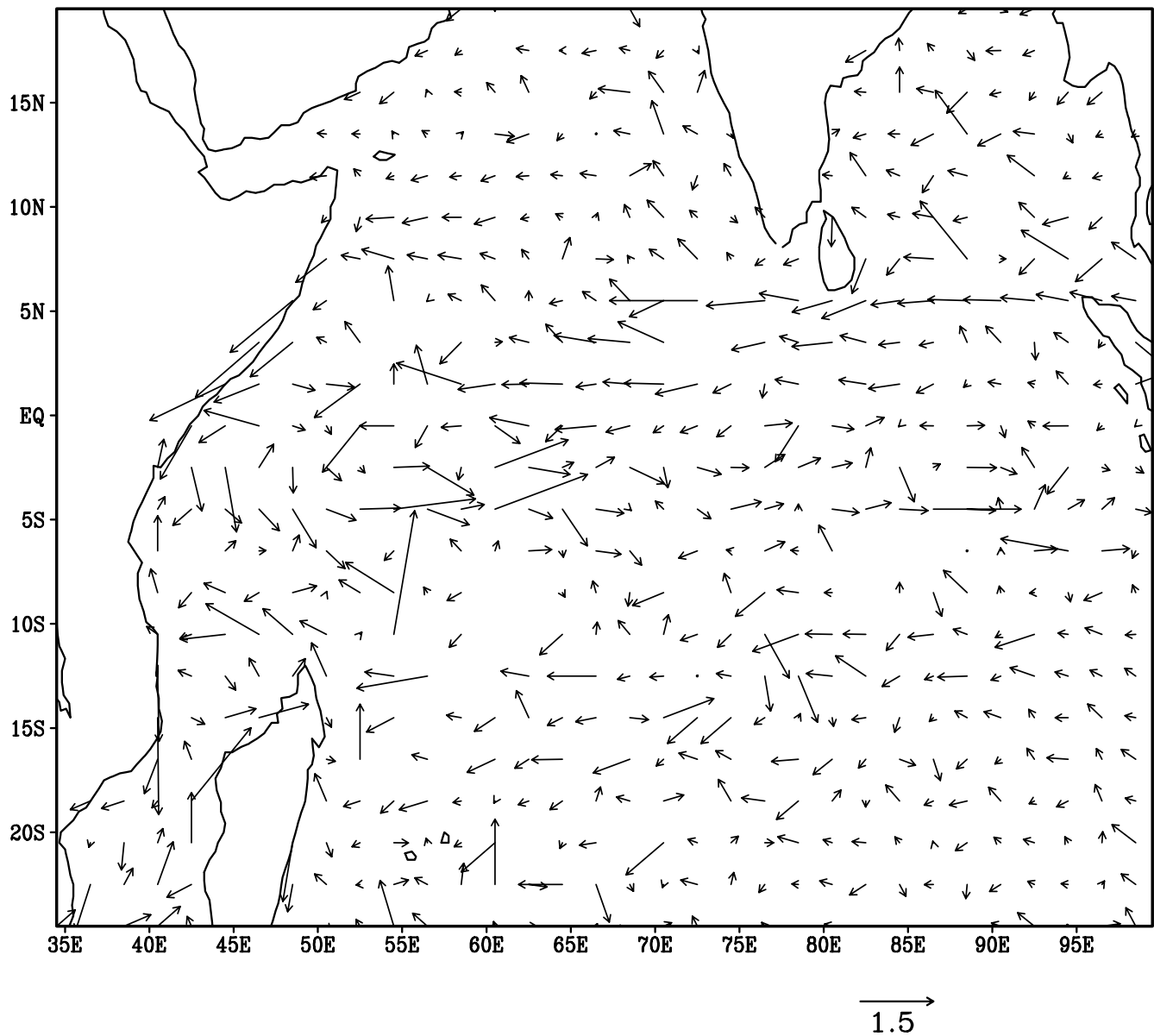


Fig.3.13. Ship drift surface currents (m/s) of Cutler and Swallow (1984)  
for the month of January



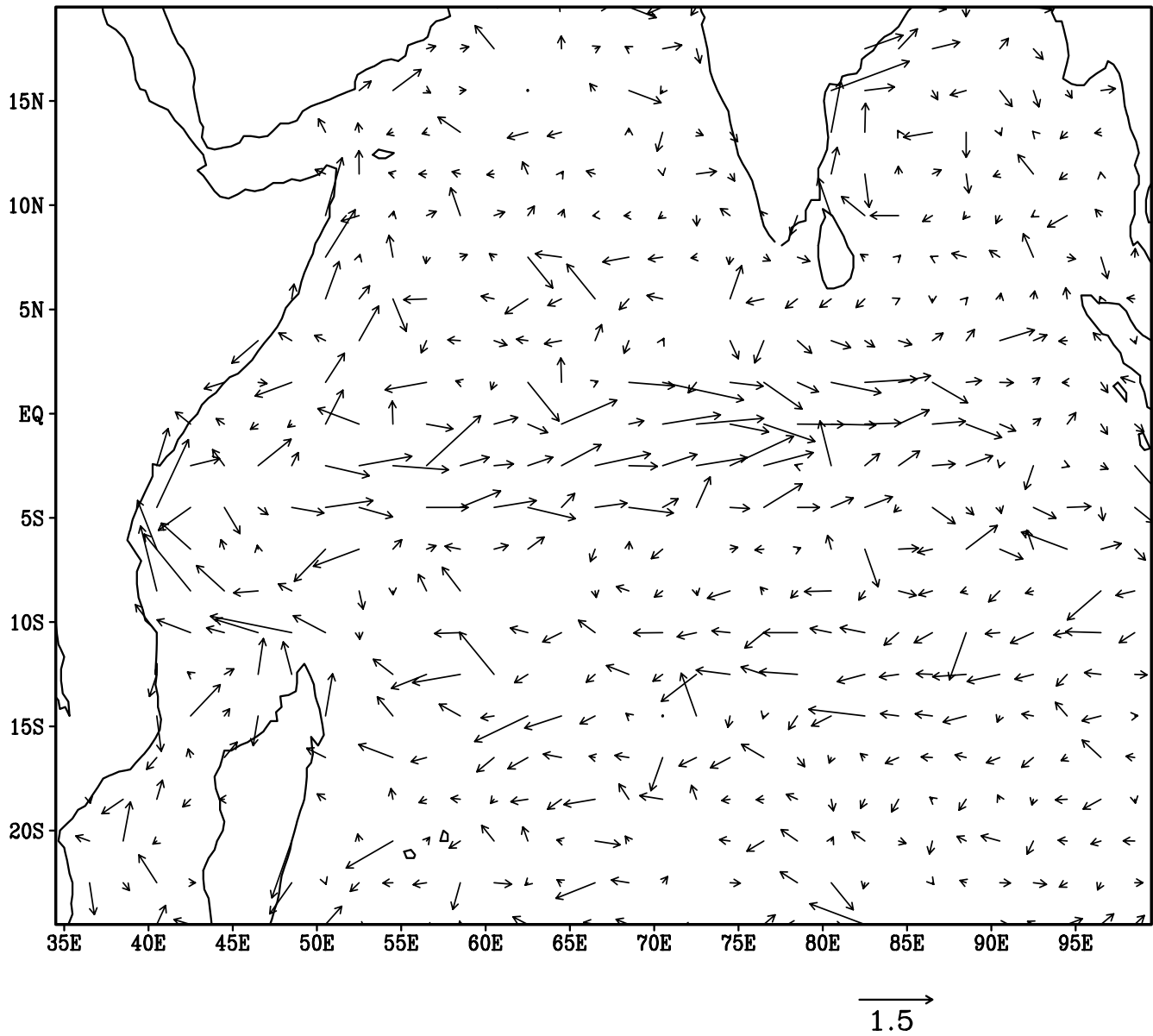


Fig.3.14. Ship drift surface currents (m/s) of Cutler and Swallow (1984)  
for the month of April

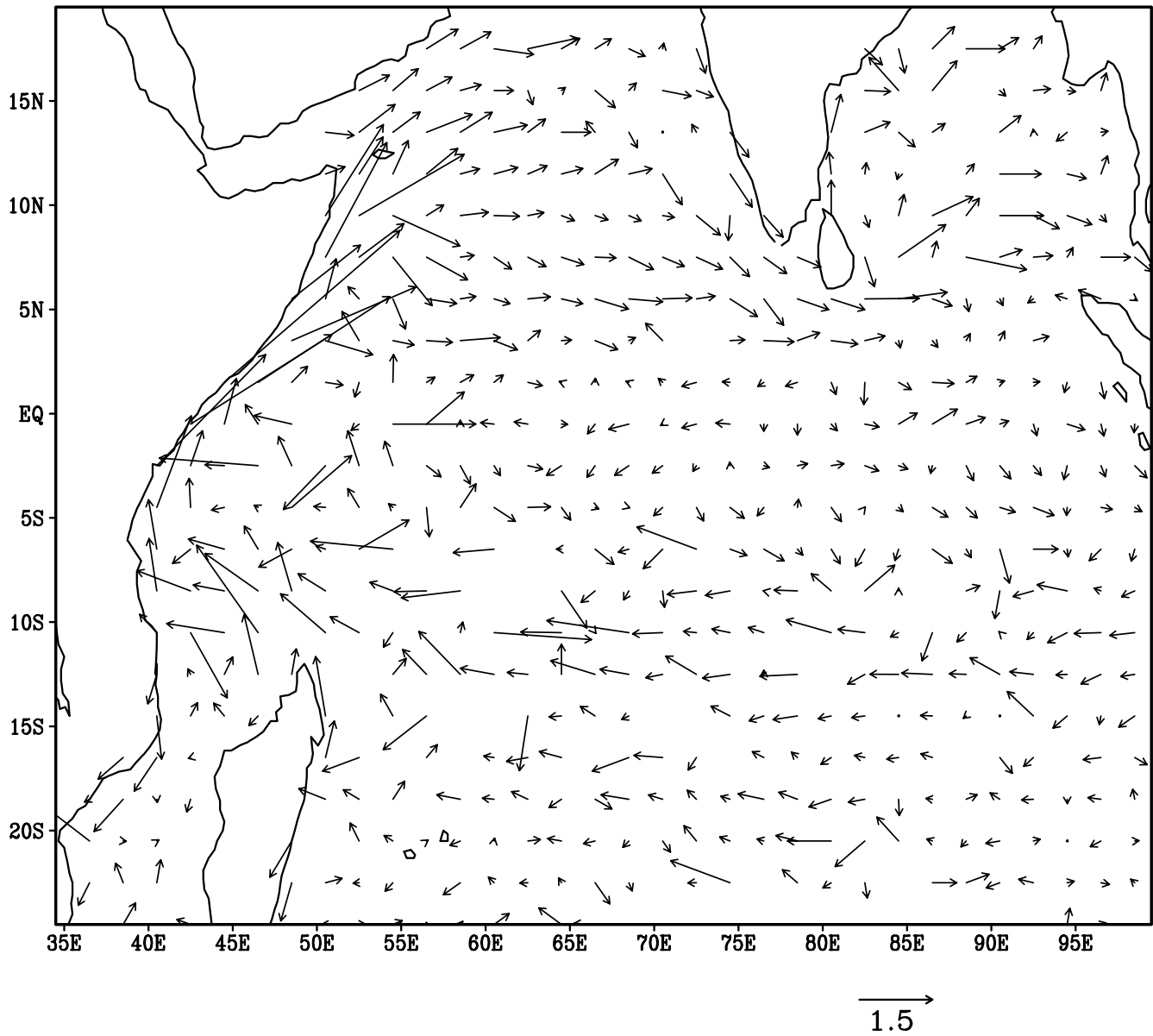


Fig.3.15. Ship drift surface currents (m/s) of Cutler and Swallow (1984)  
for the month of July

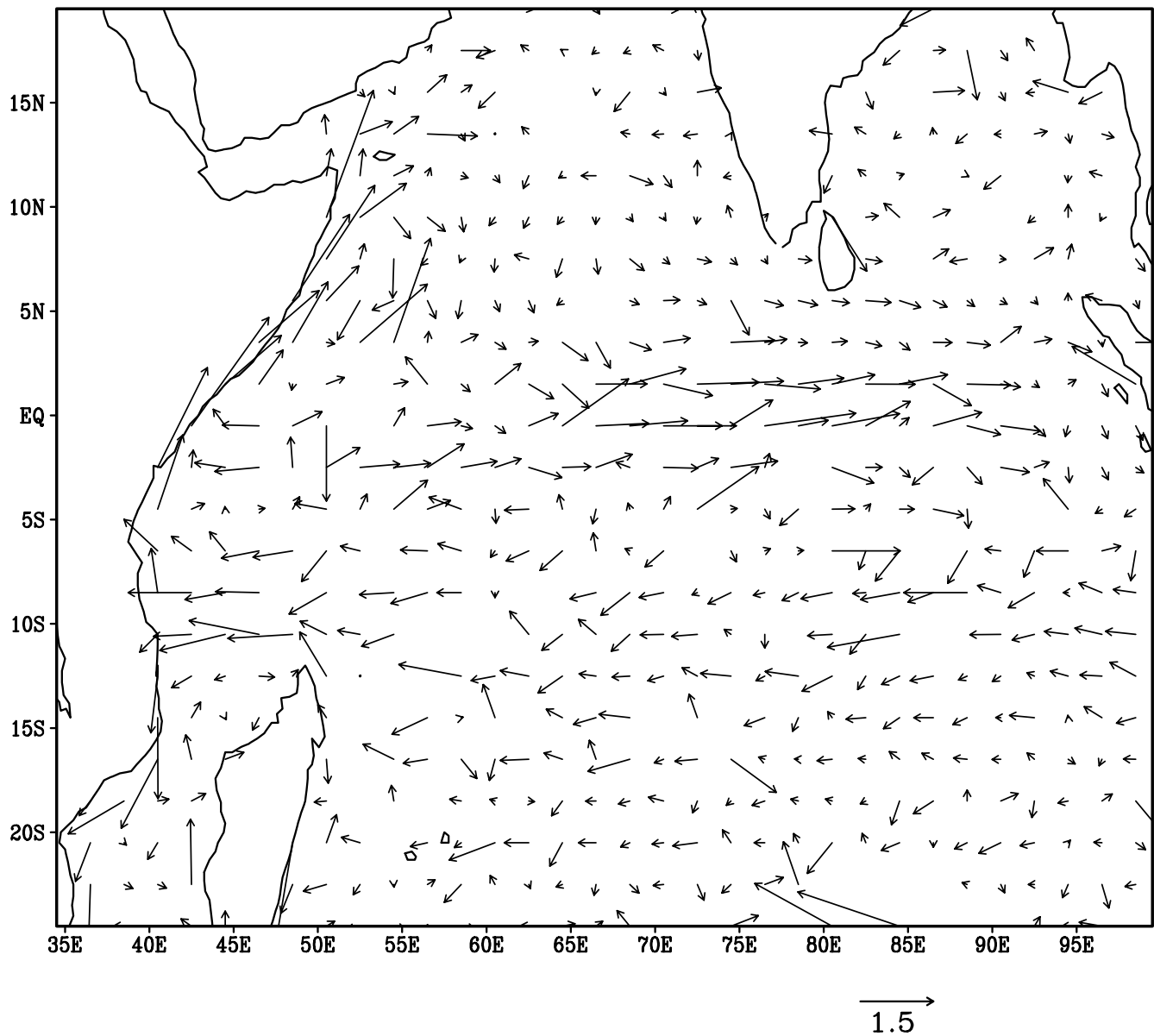


Fig.3.16. Ship drift surface currents (m/s) of Cutler and Swallow (1984)  
for the month of October

there is a northward flow north of 10°N and a southward flow south of it. The magnitude of EICC during July is approximately of the order of 30 cm s<sup>-1</sup> (Fig. 3.3 b-c). The probable reasons for the northward surface EICC north of 10°N and southward EICC to the south of 10°N can be given in terms of the prevailing wind stress curl pattern over the western Bay of Bengal. During summer, the wind stress curl is cyclonic in the southwestern part of the Bay of Bengal and this cyclonic curl drives a southward flow south of 10°N. Ship drift data show that the northward surface EICC starts just north of Sri Lanka at about 8°N and there is a southward surface EICC all along the Sri Lankan coast. The ship drift data do not show a well defined anticyclonic type of circulation in the Bay of Bengal. Our model results agree with the studies of Eigenheir and Quadfasel (2000) who found that the surface EICC flow northward to the north of 10°N and southward south of 10°N.

The poleward flowing EICC is a continuous current at the subsurface levels of 50 m and 150 m depths and is mainly driven by thermohaline forcing. There is a steady increase in the temperature field from west to east creating an upward slope of the sea surface in the same direction. Such a slope of sea surface can generate a poleward subsurface EICC during July (Fig. 3.9a-b). Low saline water watermass is found in the central Bay of Bengal during July (Figs. 3.10a-b).

During the month of October, weak winds prevail over the entire Bay of Bengal except off Sri Lankan coast. A weak southward flowing EICC was reproduced by the semi-diagnostic model and could be seen only very near to the coastline. Small cyclonic type of circulation cells were observed in the western Bay of Bengal, while southerly flows were observed in the central Bay of Bengal (Figs. 3.4a-b). At 150 and 300 m depths, anticyclonic type of circulation with magnitude ranging from 5 to 10 cm s<sup>-1</sup> was noticed (Fig. 3.4 c-d). The semi-diagnostic model could not reproduce the fairly strong southward flowing EICC as observed in the

ship-drift data. It may be due to the absence of remote forcing effects in the model dynamics. So can be suggested that the remote forcings play a major role in the circulation of Bay of Bengal during October. In the month of October, no significant gradients in the temperature-salinity characteristics were noticed in the upper layers of Bay of Bengal (Fig. 3.4a-b and 3.12a-b).

### **3.4.3 Spatial variability of monthly mean currents in the upper layers of equatorial and southern tropical Indian Ocean**

The wind field that drives the equatorial Indian Ocean is unique in that its annual mean is weak and westerly and its annual cycle has a strong semi-diurnal component. Shipdrift climatology of Cutler and Swallow (1984) indicates that surface currents in the equatorial Indian Ocean reverse direction four times a year, flowing westwards during winter, weakly westwards in the central and western ocean during summer and strongly eastward during spring and fall. The strong eastward current currents are known as Wyrtki jets or Equatorial Jets. These jets are directly forced by the semi-annual component of winds as pointed out by Han et al. (1999).

In the southern Indian Ocean south of 10°S, the winds are southeasterly throughout the year. Although, the monsoonal forcing is prominent in the northern Indian Ocean, the southern subtropical and mid latitude Indian Ocean also undergoes seasonal variability related to monsoons. The South Equatorial Current (SEC) is the most powerful, perennial current system in the southern tropical Indian Ocean. Ship drift currents (Cutler and Swallow, 1984) and drifter tracks (Shenoi et al. 1999) show SEC as a band of westward flow between 10°S and 20°S that extends across the basin. This current is mainly driven by the prevailing southeast trades which provide the major mechanical forcing for the basin wide upper ocean circulation in the southern tropical Indian Ocean. The SEC splits along the east coast of Madagascar around 17°S generating the North East Madagascar Current (NEMC) and South East Madagascar Current

(SEMC). The SEC on reaching the east African coast feeds the East African coastal current (EACC) which flows northward throughout the year with a mean speed of  $40 \text{ cm s}^{-1}$ . At the western boundary during the northeast monsoon season, the northward EACC and southward SC cause a confluence at  $3-5^{\circ}\text{S}$  and merges to form the eastward flowing counter current known as South Equatorial Counter Current.

Semi-diagnostic model solution for the month of January (Fig. 3.1c) shows that the SEC flows primarily towards west with a magnitude of approximately  $30 \text{ cm s}^{-1}$  between  $10^{\circ}\text{S}$  and  $20^{\circ}\text{S}$ . The model SEC splits along the east coast of Madagascar at approximately  $15^{\circ}\text{S}$  with one branch flowing northward (NEMC) and the other branch flowing towards south (SEMC). The model SEC on reaching the East African coast feeds the East African Coastal Current (EACC) which flows northward throughout the year with a magnitude of approximately  $40 \text{ cm s}^{-1}$ . As observed, the model EACC meets the southward flowing Somali Current (SC) at the equator, merging together and to flow eastward as counter current known as South Equatorial Counter Current (SECC). The SECC is well reproduced in the model with a magnitude of  $30 \text{ cm s}^{-1}$ . The computed results at the surface fully agree with shipdrift data compiled by Cutler and Swallow (Fig. 3.13). The SEC, EACC and SECC could be traceable at 50 m depth. The Equatorial circulation at 150 and 300 m depths is dominated by the presence of a strong eastward flowing Equatorial Undercurrent (EUC) between the latitudes  $5^{\circ}\text{N}$  and  $5^{\circ}\text{S}$ . The magnitude of this eastward flowing EUC varies between  $20 \text{ cm s}^{-1}$  and  $30 \text{ cm s}^{-1}$ . EACC, SEMC and NEMC are still clearly visible at both 150 and 300 m depths (Figs. 3.1 c-d). The currents at other regions of southern tropical Indian Ocean is considerably weak during January. The Equatorial undercurrent was first documented by Taft (1967) at several locations along the equator between  $56^{\circ}\text{E}$  and  $91^{\circ}\text{E}$  during March-April of 1963. The Equatorial Undercurrent is primarily driven by the east-west slope caused by the prevailing easterlies. Swallow et al. (1983) studied

the boundary currents east and north of Madagascar using current measurements and temperature and salinity data and found that the SEC splits into two at approximately 17°S at the east coast of Madagascar forming SEMC and NEMC. Both these branches of SEC are reproduced by the model and could be seen at 150 m and 300 m depths.

Model solutions at the surface and 50 m depths for the month of April are presented in Fig. 3.2a-b. In the month of April, a weak westward flowing North East Monsoon Current (NEMC) could be seen between the Equator and 10°N. The striking feature observed in the equatorial region during April is the appearance of a broad eastward current known as Wyrтки Jet (WJ). Wyrтки Jet could be traced across the Equatorial regions between 2°S and 2°N latitude and its magnitude varies between 20 cm s<sup>-1</sup> and 30 cm s<sup>-1</sup>. The model Wyrтки Jet could be seen both at the surface and 50 m depth. All the permanent currents in the southern tropical Indian Ocean such as SEC, EACC, NEMC and SEMC during April were reproduced by the model. The WJ become weaker at 150 m depth and could be traced only upto central Equatorial Indian Ocean. Another important finding during April is that the EACC flows north-northeastward with a speed of approximately 25 cm s<sup>-1</sup> even at 150 and 300 m depths.

The model solution for the month of July shows that the SEC flows south of westwards across the entire southern tropical Indian Ocean between the latitudes 10°S and 20°S. The magnitude of SEC during July is stronger as compared to winter season, and its magnitude varies between 40 cm s<sup>-1</sup> and 60 cm s<sup>-1</sup>. A large anticyclonic gyre was found in the western equatorial Indian Ocean between 15°S and equator. Another important finding during the month of July is the appearance of EUC that flows eastward in the equatorial belt at 50, 150 and 300 m depths. The SEC feeds into the Somali current via EACC and its magnitude is considerably reduced at 300 m depth. The computed subsurface circulation in the tropical Indian Ocean generally agree with the ship drift

data compiled by Cutler and Swallow (1984) and the existing observations in the Indian Ocean region. The semi-diagnostic model has been successful in reproducing all the permanent current systems in the Indian Ocean including the undercurrents.

### **3.5 Forcing Mechanisms and Conclusions**

In this chapter, a primitive equation type, sigma coordinate, 3-dimensional semi-diagnostic circulation model has been used to study the relative roles of steady local forcing of wind and internal density field on the general circulation of Indian Ocean. The spatial variability of mean currents in the upper layers of Arabian Sea, Bay of Bengal, Equatorial and southern tropical Indian Ocean were presented under separate headings.

#### **(I) Circulation in the Arabian Sea**

Model calculations for the month of January showed that the westward flowing north equatorial current (North East Monsoon Current) was present in the latitudinal belt (2°N - 6°N), and it impinged on the Somali coast with one branch flowing towards north-northeast and the other branch flowing southwestwards along the Somali coast as Somali Current (SC). The model reproduced the northward flowing East African Coastal Current (EACC) and the West India Coastal Current (WICC) present during the winter season (January); however, the Socotra eddy could not be reproduced by the model because of the model's low resolution. All the major surface currents were discernable at 50 m depth also, but the strength of the current was considerably reduced.

Model calculations on mean currents in the upper layers for the month of April showed that the westward flowing northeast monsoon current (NMC) was present in the latitudinal belt 5°N - 10°N, but its intensity was considerably reduced as compared to January month. A clear anticyclonic circulation consistent with the prevailing wind field was noticed in the entire



northern Arabian Sea. Model reproduced a weak equatorward flowing WICC all along the west coast of India in the upper 50 m water column.

Model calculations for the month of July showed the presence of northeastward flowing Somali current, the southern gyre (SG) and the Great Whirl (GW). The Somali Current (SC) was found to be an extension of EACE which flows northward across the equator. In the semi-diagnostic calculations, only the local forcings of wind stress and internal density fields were considered and it reproduced fully the gyres in the Somali current system. It is, therefore, inferred that the Somali current system is mainly forced by the alongshore wind associated with the Findlater Jet and the internal density field. The southwest monsoon current (SMC) was found to be primarily wind-driven, although the influence of density gradient on the strength and direction could be seen to a certain extent. The model calculation showed the presence of WICC along the west coast of India during July and its presence could be seen upto 50 m depth.

During the month of October, the northeastward flowing Somali current including the clockwise eddy found off the Somali coast were reproduced by the model. These results were comparable to shipdrift observations. A clear cyclonic circulation which could be seen at the surface and 50 m depth was found in the central Arabian Sea during the month of October.

## **(ii) Circulation in the Bay of Bengal**

Model calculations on currents in the Bay of Bengal during January showed that a large anticyclonic gyre was found in the entire Bay of Bengal north of 8°N. The East India Coastal Current (EICC) associated with the wind-driven anticyclonic gyre in the Bay of Bengal flowed poleward all along the East Coast of India. It was inferred that combined effect of local wind forcing and thermal structure are responsible for the observed circulation in the Bay of Bengal during January.

The EICC flows poleward along the East Coast of India during April and the model computed EICC features broadly agree with the ship drift data. It is found that the wind-driven EICC is part of an anticyclonic gyre formed in the Bay of Bengal during January-May and is best developed during April. Both thermohaline forcing and wind stress fields are responsible for the formation of poleward flowing EICC during April.

During July, the EICC does not flow poleward as expected along the east coast of India. Model results showed that there was a northward flow north of 10°N and a southward flow south of it. The probable reason for the northward surface EICC north of 10°N and a southward EICC south of it can be given in terms of the prevailing wind stress curl pattern. During summer, the wind stress curl is cyclonic in the south western part of Bay of Bengal and this cyclonic curl could drive a southward flow south of 10°N. The poleward flowing EICC is a continuous current at the subsurface levels of 50 m and 150 m depths.

During the month of October, a weak southward flowing EICC was reproduced by the semi-diagnostic model very near to the coastline. Small cyclonic type of circulation cells were observed in the western Bay of Bengal, while southerly flows were observed in the central Bay of Bengal. The semi-diagnostic model could not reproduce the fairly strong southward flowing EICC as observed in the shipdrift data. We believe that this could be due to the absence of remote forcing effects in the model dynamics.

### **(iii) Mean currents in the equatorial and southern tropical Indian Ocean**

The semi-diagnostic model calculation for the month of January showed that the South Equatorial Current (SEC) flowed primarily towards west with a magnitude of approximately  $30 \text{ cm s}^{-1}$  between 10°S and 20°S. As observed, the model SEC splits along the east coast of Madagascar at

15°S with one branch flowing northward as North East Madagascar Current (NEMC) and the other branch flowing southward as South East Madagascar Current (SEMC). The model SEC feeds the East African Coastal Current (EACE) on reaching East African coast. The South Equatorial Counter Current (SECC) was well reproduced by the model. The computed results agree with the shipdrift data compiled by Cutler and Swallow (1984). The Equatorial circulation at 150 and 300 m depths is dominated by the presence of a strong eastward flowing Equatorial Undercurrent (EUC) between the latitudes 5°N and 5° S.

The model solutions at the surface and 50 m depths for the month of April showed a weak westward flowing North East Monsoon Current (NEMC) and a strong eastward current known as Wyrтки Jet (WJ). The Wyrтки Jet could be traced across the equatorial regions between 2°S and 2°N and its magnitude varies between 20 cm s<sup>-1</sup> and 30 cm s<sup>-1</sup>. All the permanent currents in the southern tropical Indian Ocean such as SEC, EACE, NEMC and SEMC during April were reproduced by the model.

Model solution for the month of July showed that SEC flowed south of westward across the entire southern tropical Indian Ocean between 10°S and 20°S. Another important finding during the month of July is the appearance of EUC that flows eastward in the equatorial belt at 50, 150 and 300 m depths.

The semi-diagnostic model has been successful in reproducing all the permanent current systems in the Indian Ocean including undercurrents over the entire annual cycle.